

Regiodivergent Organocatalytic Reactions

Mayavan Viji, Srinu Lanka, Jaeuk Sim, Chanhyun Jung, Heesoon Lee, Manjunatha Vishwanath * and Jae-Kyung Jung *

College of Pharmacy and Medicinal Research Center (MRC), Chungbuk National University, Cheongju 28160, Korea; cheviji@gmail.com (M.V.); lsrinu23@gmail.com (S.L.); simprog@naver.com (J.S.); cksgus9823@naver.com (C.J.); medchem@cbnu.ac.kr (H.L.)

* Correspondence: 16vishwanath@gmail.com (M.V.); orgkjung@chungbuk.ac.kr (J.-K.J.); Tel.: +82-43-261-2635 (J.-K.J.); Fax: +82-43-268-2732 (J.-K.J.)

Abstract: Organocatalysts are abundantly used for various transformations, particularly to obtain highly enantio- and diastereomeric pure products by controlling the stereochemistry. These applications of organocatalysts have been the topic of several reviews. Organocatalysts have emerged as one of the very essential areas of research due to their mild reaction conditions, cost-effective nature, non-toxicity, and environmentally benign approach that obviates the need for transition metal catalysts and other toxic reagents. Various types of organocatalysts including amine catalysts, Brønsted acids, and Lewis bases such as N-heterocyclic carbene (NHC) catalysts, cinchona alkaloids, 4-dimethylaminopyridine (DMAP), and hydrogen bond-donating catalysts, have gained renewed interest because of their regioselectivity. In this review, we present recent advances in regiodivergent reactions that are governed by organocatalysts. Additionally, we briefly discuss the reaction pathways of achieving regiodivergent products by changes in conditions such as solvents, additives, or the temperature.

Keywords: organocatalysts; regiodivergent; metal-free; Lewis base; NHC; amine catalyst; Brønsted acid; hydrogen bond-donating catalysts; solvent control; temperature control

Citation: Viji, M.; Lanka, S.; Sim, J.; Jung, C.; Lee, H.; Vishwanath, M.; Jung, J.-K. Regiodivergent Organocatalytic Reactions. *Catalysts* **2021**, *11*, 1013. <https://doi.org/10.3390/catal11081013>

Academic Editor: Moris S. Eisen

Received: 8 July 2021

Accepted: 20 August 2021

Published: 22 August 2021

Publisher's Note: MDPI stays neutral with regard to jurisdictional claims in published maps and institutional affiliations.



Copyright: © 2021 by the authors. Licensee MDPI, Basel, Switzerland. This article is an open access article distributed under the terms and conditions of the Creative Commons Attribution (CC BY) license (<http://creativecommons.org/licenses/by/4.0/>).

1. Introduction

Over the past two decades, reactions that rely on organocatalysts have emerged as important catalytic systems in asymmetric and conventional synthesis [1–14]. The utilization of organocatalysts has garnered interest because they are robust, inexpensive, environmentally benign, and easily recoverable, among other advantageous characteristics. Moreover, the use of chiral organic molecules as catalysts enables the synthesis of highly enantio- and diastereomeric pure products, which are of great importance in medicinal and pharmaceutical chemistry [15–18].

Controlling the selectivity of the reactions is one of the popular fields of the research area in synthetic organic chemistry. Organocatalysts have made it possible to develop a large number of reactions to synthesize stereoselective [19–29], regioselective [30–40], and chemo-selective [41–48] products. Regiodivergent synthesis reactions, which enable two or more regioisomeric products to be synthesized from the same starting material, are controlled by various reaction parameters such as catalysts, additives, solvents, temperatures, ligands, and functional groups [49,50]. Although several metal-catalyzed regiodivergent reactions have been thoroughly studied [51–55], organocatalytic regiodivergent reactions have not been explored [56]. This mini review of organocatalytic regiodivergent reactions is intended to fill this void.

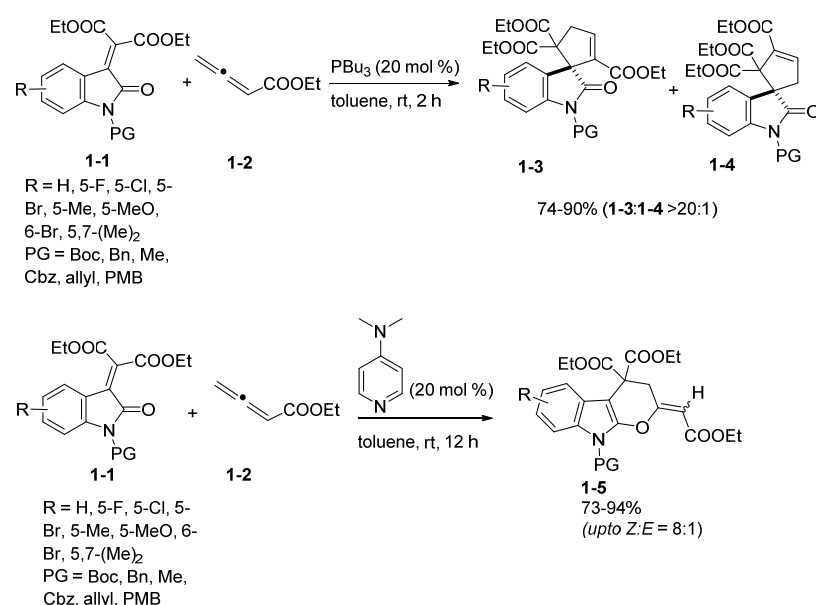
2. Lewis Base Catalysts

Lewis base catalysts, including various tertiary amines (1,8-diazabicyclo[5.4.0]undec-7-ene (DBU), 4-dimethylaminopyridine (DMAP), 1,4-diazabicyclo[2.2.2]octane (DABCO), etc.), cinchona alkaloids, and *N*-heterocyclic carbene (NHC) catalysts, are widely utilized for asymmetric transformations such as the aldol reaction, the Morita–Baylis–Hillman reaction, and cycloaddition. One primary application of this type of catalyst is formal cycloaddition reactions, in which this catalyst type combines with ketenes or alkynes to form in situ generated zwitterion. These intermediates subsequently undergo a cycloaddition reaction with several electrophilic moieties to yield the cyclized products. Consequently, various types of cycloaddition reactions have been developed such as [2+2], [2+3], and [2+4] [57–66].

2.1. Phosphine and Amine Bases

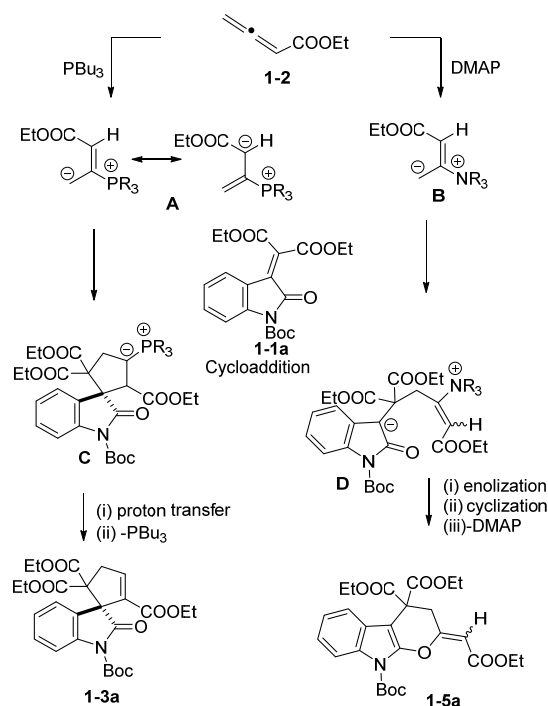
Recently, nucleophilic phosphine- and nitrogen-containing Lewis bases have emerged as a powerful tool for constructing carbo- and heterocyclic compounds under metal-free and mild reaction conditions. Several natural products and spirocyclic compounds were synthesized by using these catalysts via a cycloaddition reaction with allenates or alkynones. In general, these reactions occur by way of cycloaddition of the allenates with electron-deficient olefins or imines via [3+2] and [4+2] cycloadditions [57–66].

Shi's group developed a highly regioselective [3+2] cycloaddition reaction by using phosphine as a Lewis base, which afforded five-membered spiro compounds (Scheme 1) [67]. The cycloaddition reaction was conducted between an α -allenic ester (**1-2**) and α,β -unsaturated diesters (**1-1**) which derived from isatin, in the presence of PBu_3 , and the reaction proceeded smoothly by way of a [3+2] cycloaddition to yield **1-3** and **1-4** in >20:1 regioselectivity. With different electron-donating groups (EDGs), or electron-withdrawing groups (EWGs), at the fifth, sixth, or seventh positions, the reaction proceeded without complication to furnish the products in good yields. In contrast, the DMAP-catalyzed reactions initiated [4+2] cycloadditions to yield the six-membered dihydropyranone products **1-5**. Various isatins having different EDGs and EWGs on the benzene rings and different *N*-protecting groups underwent this cycloaddition reaction depending on the catalyst used to afford the desired cyclic products in good yield with good geometric selectivities.



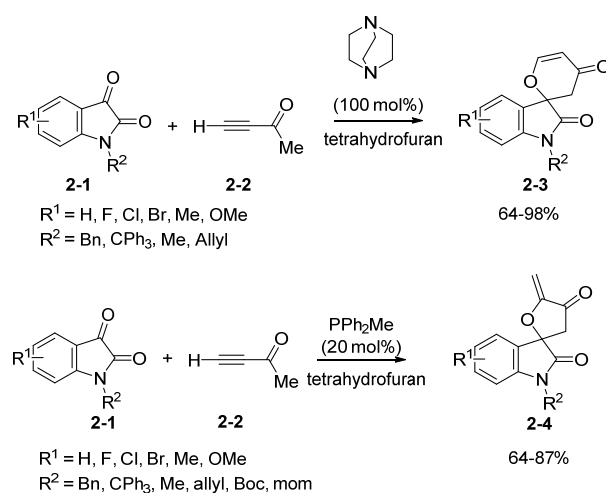
Scheme 1. Lewis base-catalyzed [3+2] and [4+2] cycloaddition reactions.

The proposed reaction mechanism is depicted in Scheme 2. The reaction commences with the addition of a phosphine catalyst to the allenic ester (**1-2**) to produce a zwitterionic intermediate. The intermediate serves as a dipole for the subsequent [3+2] cycloaddition, which occurs at the C-3 position of isatin to produce intermediate **C**. Subsequently, 1,2-proton transfers followed by regeneration of the catalyst afford product **1-3a**. In the case of DMAP, a zwitterionic intermediate forms by the addition of the base DMAP to the allenic ester, which reacts with **1-1a** to produce intermediate **D**. Consecutive enolization, followed by cyclization and elimination of the catalyst, delivers the six-membered dihydropyranone **1-5a** products.

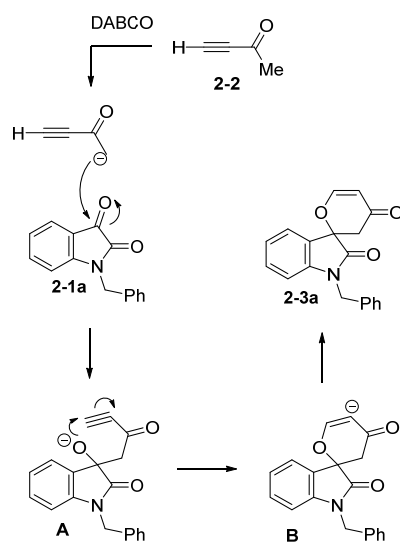


Scheme 2. Proposed mechanism for [3+2] and [4+2] cycloaddition reactions.

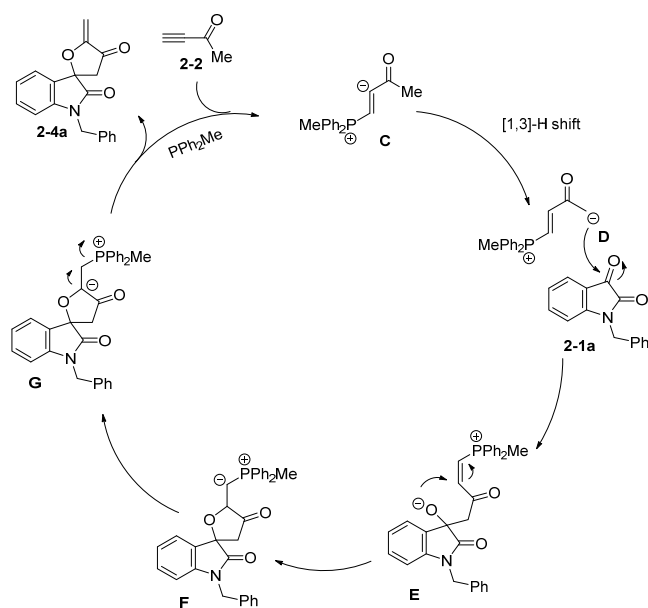
In their continuous efforts in this study, Shi *et al.* demonstrated different cycloaddition reactions in which different regiodivergent spiro compounds were obtained depending on the Lewis bases involved in the reaction (Scheme 3) [68]. In the presence of nitrogen-containing base DABCO, isatin (**2-1**) reacts with butynone (**2-2**) to produce six-membered spiro compounds, the pyranones (**2-3**). With isatins bearing either EWG or EDG substituents at various positions on the benzene ring, the reaction proceeded smoothly to afford the products in good yield. On the other hand, the use of PPh₂Me as a Lewis base promoted the formation of the five-membered spiro compound furanone (**2-4**). Optimized conditions applied with various EWG and EDG groups on the benzene ring had no influence on the reaction yields. Various protecting groups on nitrogen underwent the reaction smoothly to yield five-membered oxygen-containing spiro compounds in moderate to good yields. Focusing on the mechanistic study, initial deprotonation of butynone generates an enolate intermediate in the presence of DABCO (Scheme 4). Later, nucleophilic addition is followed by an intramolecular Michael addition of an O[−] anion to the alkynyl group, and protonation to yield the required six-membered pyranone product (**2-3**). Using PPh₂Me with butynone initially generates a zwitterionic intermediate (**C**), which undergoes a 1,3-hydrogen shift to form an enolate intermediate (**D**). Nucleophilic addition to the carbonyl group followed by intramolecular addition of an O[−] anion (**E**) to the alkenyl group creates the desired five-membered spiro products (**2-4**) by the liberation of the catalyst (Scheme 5).



Scheme 3. Synthesis of spiro-cyclohexanoxindole and spiro-cyclopenteneoxindole.



Scheme 4. Plausible mechanism for the synthesis of pyranones (2-3).

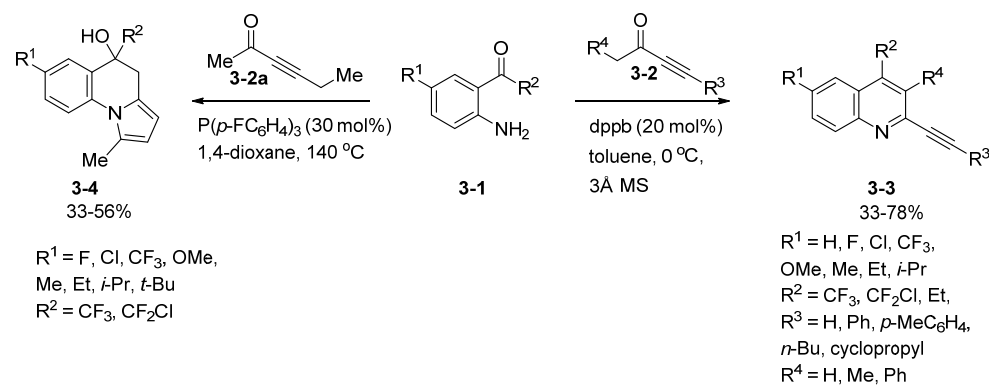


Scheme 5. Plausible mechanism for the formation of furanones (2-4).

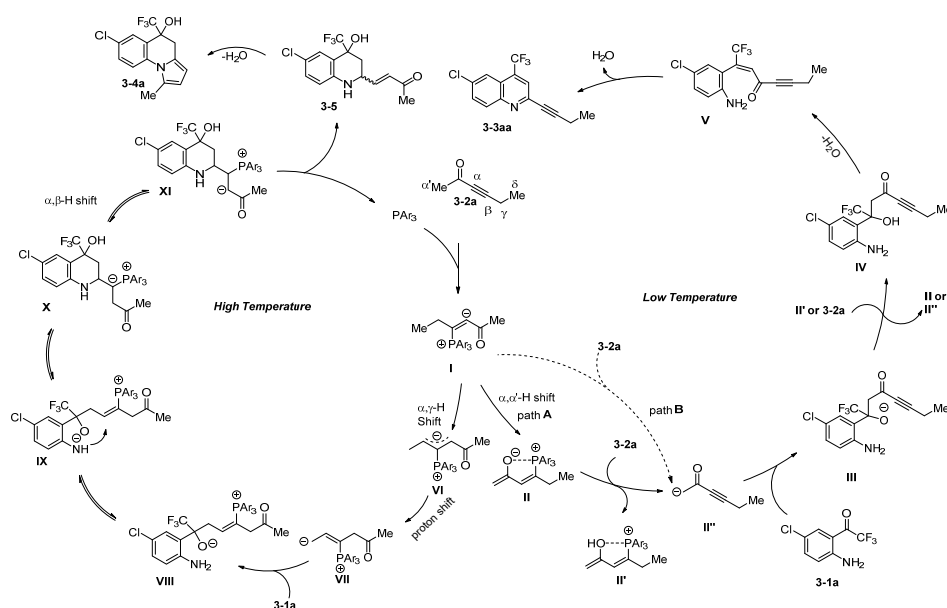
In 2019, Shi's group further explored a phosphine-catalyzed intermolecular annulation between *ortho*-aminoacetophenones and alkynes using two different regioselective approaches: [4+2] or [3+2] cycloaddition reactions (Scheme 6) [69]. Switchable transformations were achieved using different phosphine catalysts and temperatures.

Reaction between *ortho*-aminoacetophenones (**3-1**) and alkynes (**3-2**) in toluene at 0 °C in the presence of a bisphosphine catalyst such as 1,4-bis(diphenylphosphino)butane (dppb) delivered 2-alkynylquinolines (**3-3**) via a [4+2] cycloaddition reaction. This is because the lower temperatures favor the addition of phosphine to the alkyne to form zwitterionic intermediates, which then undergo an α,α -H shift, enolization, and proton abstraction to produce the α' -carbanionic species II'' (Scheme 7). This intermediate reacts with *ortho*-aminoacetophenones followed by protonation, dehydration, and intramolecular condensation to afford the quinoline products (**3-3**). This methodology exhibited a broad substrate scope that efficiently proceeded with both electron-deficient and electron-rich aromatic rings to afford the products in good yields.

Alternatively, using dioxane as the solvent and replacing the catalyst with P(*p*-FC₆H₄)₃ at an elevated temperature of 140 °C, the reaction proceeded via a [3+2] cycloaddition to provide the benzoindalazines (**3-4**). The optimized reaction conditions were effective, and the electronic factors did not have any significant impact on the reaction, which proceeded smoothly to produce the expected products in moderate yields. At a higher temperature, the zwitterionic intermediate initially underwent an α,γ -H shift followed by a proton shift to produce the δ -activated intermediate VII, which then reacted with *ortho*-aminoacetophenones followed by intramolecular proton migration, α,β -H shift, and regeneration of the catalyst to afford the compound **3-5**. Finally, the benzoindalazines (**3-4**) were obtained from compound **3-5** via the Knorr reaction methodology (Scheme 7). Both of the regioisomers were unambiguously confirmed by X-ray crystallography.

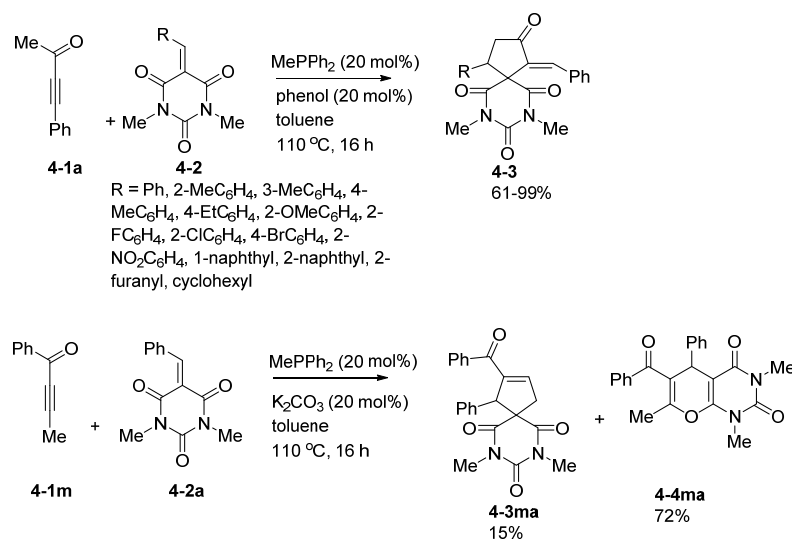


Scheme 6. Phosphine-catalyzed switchable [4+2] or [4+2]/[3+2] cycloaddition.



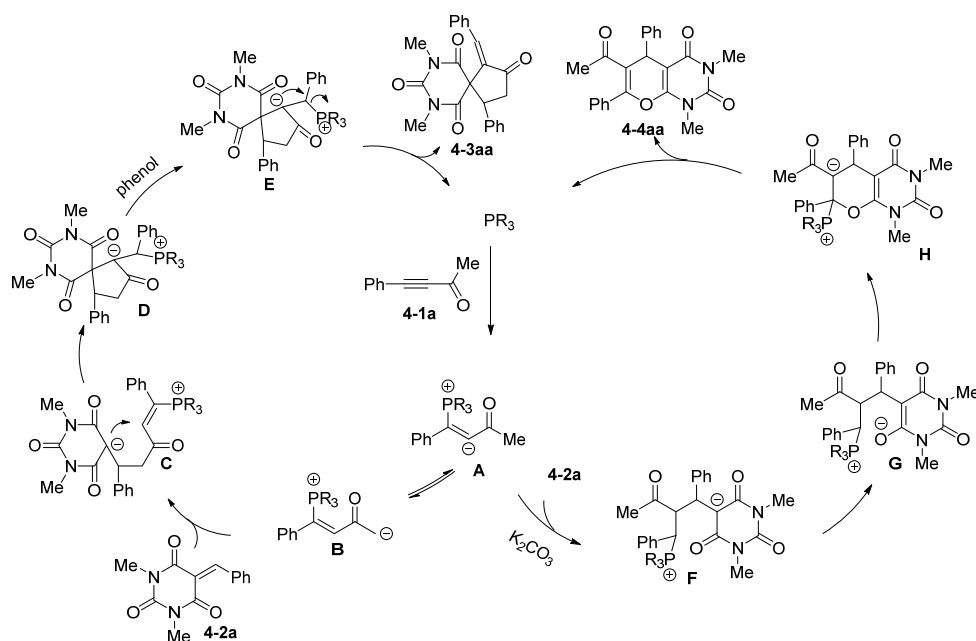
Scheme 7. Proposed mechanism for the intermolecular annulation reaction.

Guo and co-workers illustrated that a [3+2] annulation reaction between barbiturate-derived alkenes (**4-2**) and ynones (**4-1a**) would offer spirobarbiturate-cyclopentanones (**4-3**) in the presence of MePPh₂ using phenol as an acid additive (Scheme 8) [70]. Ynones containing alkyl, MeO, F, and Cl substituents were compatible with alkenes, producing the expected products in good to excellent yields, with excellent *E/Z* stereoselectivities. Similarly, the barbiturate-derived alkenes bearing various substituents including alkyl, OMe, F, Cl, Br, CF₃, CN, and NO₂ groups afforded the products in good to excellent yields. In addition to that, 1-naphthyl-, 2-naphthyl-, and 2-furanyl-derived barbiturates delivered spirobarbiturate-cyclopentanones in excellent yields. The reaction between the ynones and barbiturate-derived alkenes in the presence of MePPh₂ with an inorganic base additive, such as K₂CO₃, involved [4+2] annulation to deliver 1,5-dihydro-2*H*-pyrano[2,3-*d*]pyrimidine-2,4(3*H*)-dione (**4-4ma**) as a major product along with a minor [3+2] cycloadduct. In the absence of the phosphine catalyst, no [4+2] cycloaddition product was obtained which clearly indicates that this reaction did not occur via the hetero-Diels–Alder reaction pathway.



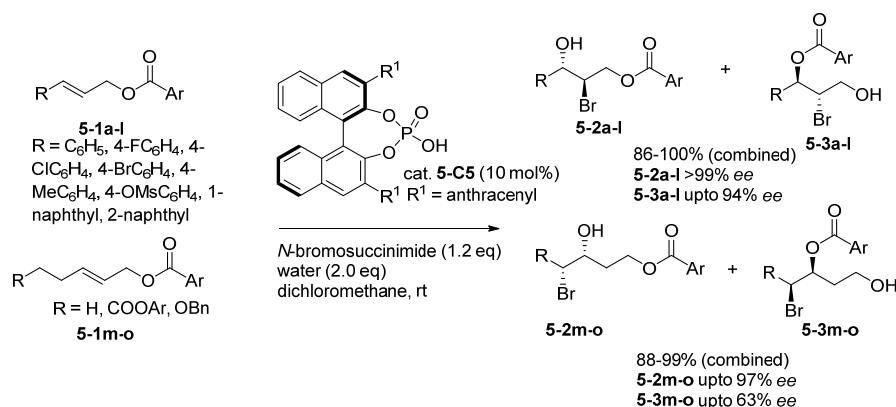
Scheme 8. Phosphine-catalyzed [3+2] and [4+2] annulation reactions.

A possible reaction mechanism is presented in Scheme 9. The phosphine catalyst initially attacks the ynone (**4-1a**) to produce intermediate **A**. In a [3+2] annulation, intermediate **A** undergoes a proton shift to produce intermediate **B**. This is followed by a conjugate addition with a barbiturate-derived alkene followed by intramolecular nucleophilic addition of the carbanion (intermediate **C**) to the double bond, which delivers the cyclic intermediate **D**. The acid additive phenol promotes 1,2-proton migration followed by regeneration of the catalyst which yields the spirobarbiturate-cyclopentanone **4-3**. In a [4+2] annulation, intermediate **A** is stabilized by the base K_2CO_3 , which produces intermediate **F** by the conjugate addition with the barbiturate-derived alkene. Intermediate **F** undergoes subsequent enolization (**G**), intramolecular oxa-Michael addition, and elimination of the phosphine catalyst to furnish 1,5-dihydro-2*H*-pyrano[2,3-*d*]pyrimidine-2,4(3*H*)-dione (**4-4**).



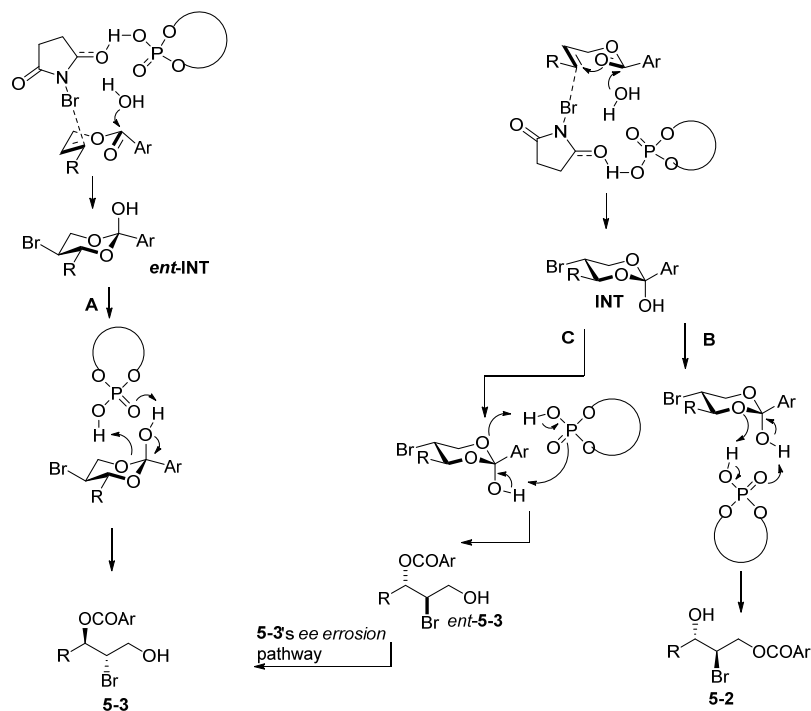
Scheme 9. Plausible mechanism for phosphine-catalyzed [3+2] and [4+2] annulation reactions.

Christmann and colleagues described the catalysis of the bromocyclization/regiodivergent reaction of alkenes (**5-1a-l**) by chiral phosphoric acids to afford both bromohydrin products in excellent yields and with good enantioselectivities (Scheme 10) [71]. More specifically, the chiral phosphoric acids containing 9-anthracenyl (**5-C5**) delivered the best results to produce both the regioisomers **5-2** and **5-3** in excellent yields with enantioselectivities. A cinnamyl ester containing an EWG or EDG in the *para* or *meta* position produced the two corresponding isomers in excellent yields with high enantioselectivities. Derivatives with sterically bulky groups such as phenyl, and 1-naphthyl derivatives at the *ortho* position smoothly reacted to afford the expected isomers in excellent yields together with good enantioselectivities. Various homoallylic esters (**5-1m-o**) were utilized to produce **5-2m-o** with excellent enantioselectivities, whereas **5-3m-o** was obtained with lower enantioselectivities.



Scheme 10. Enantioenriched bromohydrin synthesis by anchimeric oxygen borrowing.

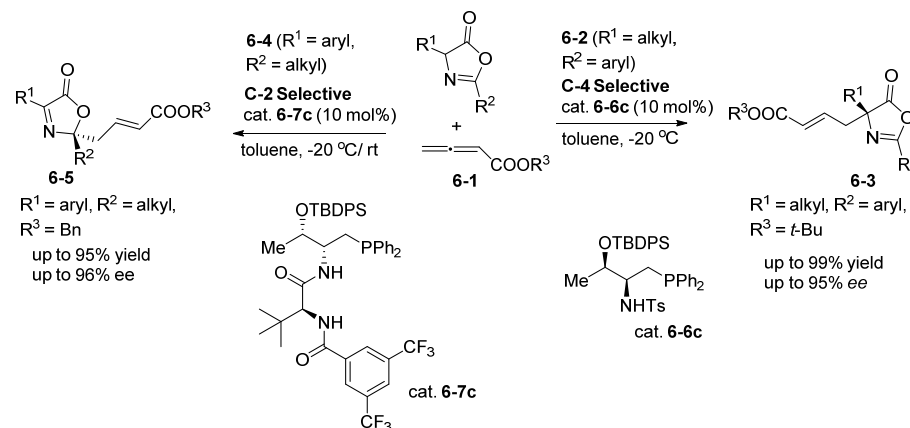
A possible mechanism for this reaction is proposed as follows (Scheme 11). Initially, the chiral phosphoric acid activates NBS for halocyclization followed by nucleophilic attack of water, affording an oxocarbenium ion, which results in both of the cyclic hemiorthoesters (INT and *ent*-INT) having excellent diastereoselectivity. At this stage, chiral phosphoric acid then collapses these intermediates for regiodivergent RRM (reaction of a racemic mixture) to afford both constitutional isomers. The authors expected that the catalyst would activate different oxygen atoms to form the respective enantiomers. INT may collapse via pathway C which results in *ent*-5-3, which may be the reason for the lower enantioselectivity of the 5-3 isomer.



Scheme 11. Proposed mechanism for the synthesis of enantioenriched bromohydrins.

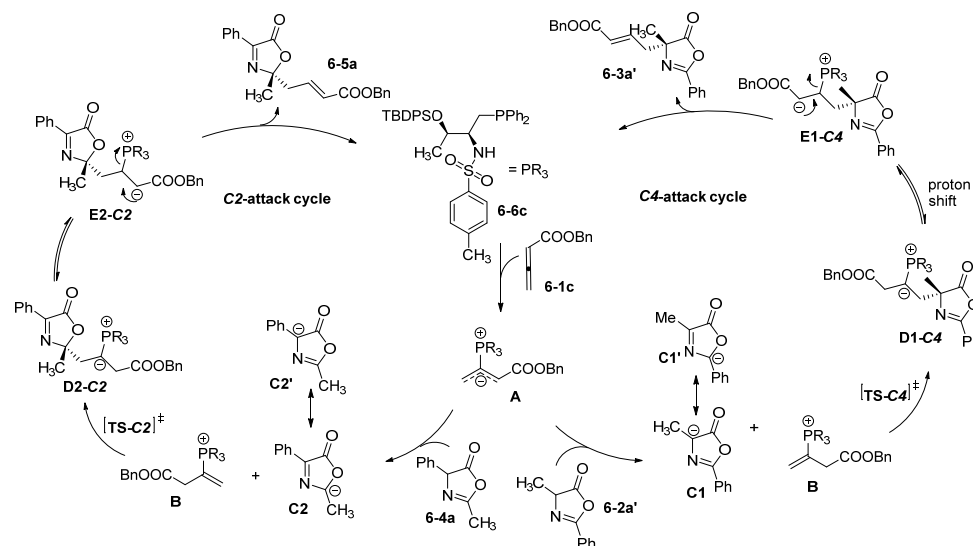
In 2016, Lu's group reported phosphine-catalyzed regiodivergent C-2- and C-4-selective γ -additions of oxazolones to 2,3-butadienoates (Scheme 12) [72]. Grafting suitable substituents on the oxazolones enabled the asymmetric C-2- and C-4-selective γ -additions of oxazolones to 2,3-butadienoates to be accomplished with excellent yields of 81 to 99% and with admirable enantioselectivities (as high as 96%) for a broad range of substrates. The C-4-selective γ -addition of oxazolones produced (6-3) in a highly enantioselective manner when 2-aryl-4-alkyloxazol-5(4*H*)-ones (6-2) were employed as pronucleophiles,

furnishing enantioenriched α,α -disubstituted α -amino acid derivatives. The employment of the 2-alkyl-4- aryloxazol-5-(4*H*)-ones (**6-4**) as the donors resulted in the C-2-selective γ -addition of oxazolones (**6-5**) in a highly enantioselective manner which led to the facile synthesis of chiral *N,O*-acetals, and γ -lactols.



Scheme 12. Phosphine-catalyzed regiodivergent enantioselective C-2 and C-4 γ -additions.

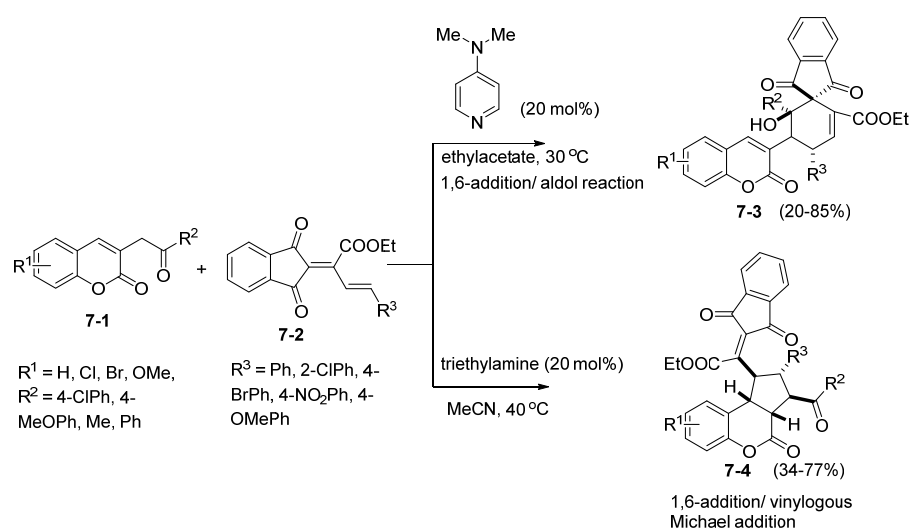
The proposed mechanistic pathway involves the formation of zwitterionic intermediate **A** by the addition of catalyst **6-6c** to **6-1c**, which then abstracts the C-4-proton of 2-phenyl-4-methyloxazol-5(4*H*)-one **6-2a'** (Scheme 13). Further oxazolidine **C1** reacts with phosphonium **B** at the C-4 position of **C1** via the transition state **TS-C4**, followed by a hydride shift to generate addition product **6-3a'** by the elimination of the catalyst. In contrast, the use of 2-methyl-4- phenyloxazol-5(4*H*)-one **6-4a** generates the oxazolidine **C2**, which favors the C-2-selective addition to eventually lead to the formation of C-2-selective product **6-5a**, via a key transition state, **TS-C2**. Theoretical studies (DFT calculations) suggested that the origin of the observed regioselectivity was the distortion energy that resulted from the interaction between the nucleophilic oxazolones and the electrophilic phosphonium intermediate.



Scheme 13. Proposed mechanism for γ -additions of oxazolone.

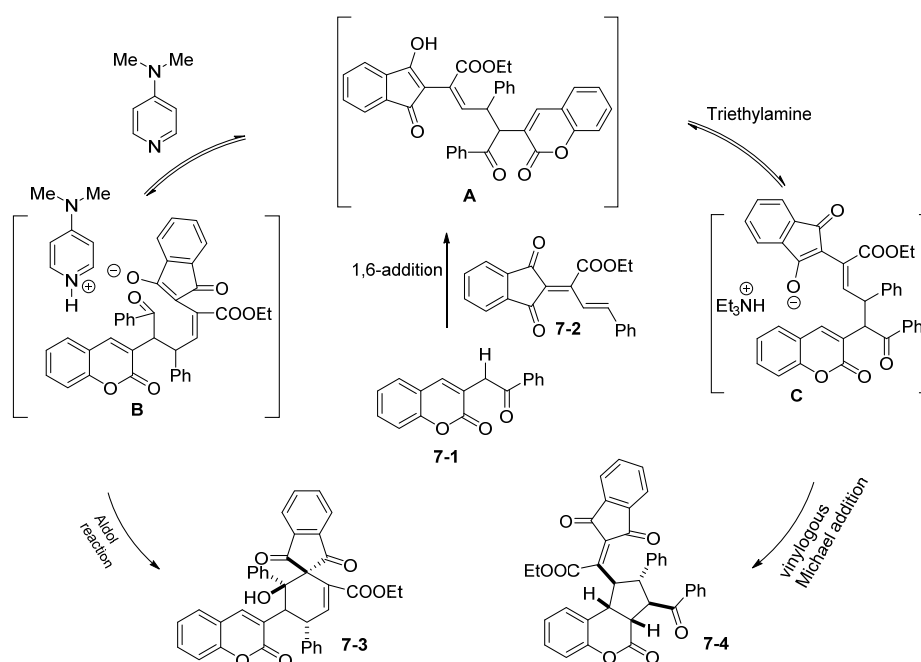
Recently, in 2020, Lin's group developed a regiodivergent cascade reaction between 3-homoacylcoumarin (**7-1**) and the 1,3-indanedione-derived 1,6-acceptor (**7-2**) to construct spirocyclohexene indane-1,3-diones (**7-3**) and coumarin-fused cyclopentanes (**7-4**) catalyzed by bases such as DMAP or Et₃N, respectively (Scheme 14) [73]. In the presence of

DMAP as the base, the reaction afforded spirocyclohexene indane-1,3-diones (**7-3**) via 1,6-addition followed by a regio- and chemoselective aldol cascade reaction. Electronic factors did not influence the yields when 3-homoacylcoumarin containing various group such as 6-Cl, 6-Br, and 6-methoxy was used, and all derivatives afforded the expected products in good yields. In the case of the indanedione-derived acceptors, EWGs provided the products in better yields than the methoxy group regardless of its position. Fused cyclopentanes (**7-4**) were obtained via 1,6-addition followed by a regio- and chemoselective vinylogous Michael addition by using Et₃N. The presence of an EWG on coumarins ensured good yields compared with an EDG irrespective of its position. This is because the EDG on coumarin enhanced the electron density at the reactive site to prevent an intramolecular Michael addition. Moreover, in the case of indanedione, sterically bulky EWGs afforded the products in good yields, whereas no product formed in the case of an EDG (OMe).



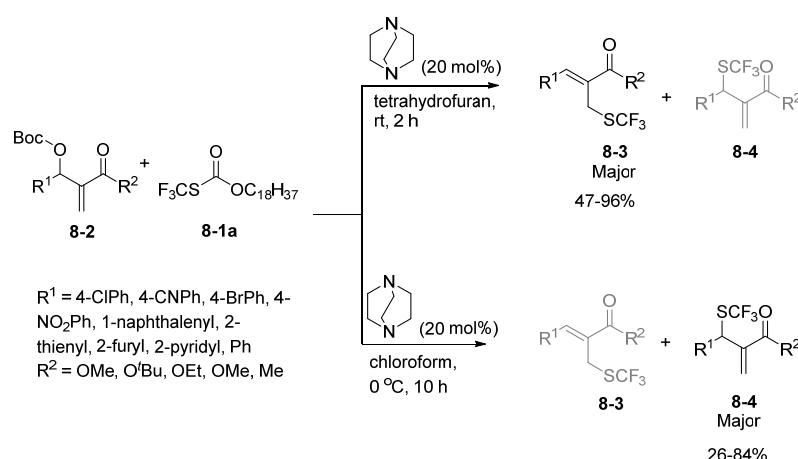
Scheme 14. Synthesis of spiro and fused systems via organobase-controlled cascade reaction.

Based on the experimental results, the authors proposed a plausible mechanistic pathway (Scheme 15). Initially, in the presence of organocatalytic bases (DMAP or Et₃N), 1,6-addition occurs between 3-homoacylcoumarin **7-1** and the indanedione **7-2** to provide a common intermediate, **A**. The conjugate acid formed by deprotonation of intermediate **A** by DMAP interacts with the dienolate to form intermediate **B**, which undergoes an intramolecular aldol reaction to deliver the desired spirocyclic product **7-3**. On the other hand, exposure of the common intermediate **A** to Et₃N forms the dienolate, which then coordinates with the respective conjugate acid to yield intermediate **C**. Finally, the intramolecular vinylogous Michael addition results in the regio- and chemoselective coumarin-fused cyclopentane **7-4**. Although the authors did not provide mechanistic proof, the selectivity was attributed to the different hydrogen bonding interactions complemented by the steric interactions with the dienolate intermediate. These interactions give rise to different transition states which result in the formation of divergent products.



Scheme 15. Plausible mechanism for organobase-controlled regiodivergent cascade reaction.

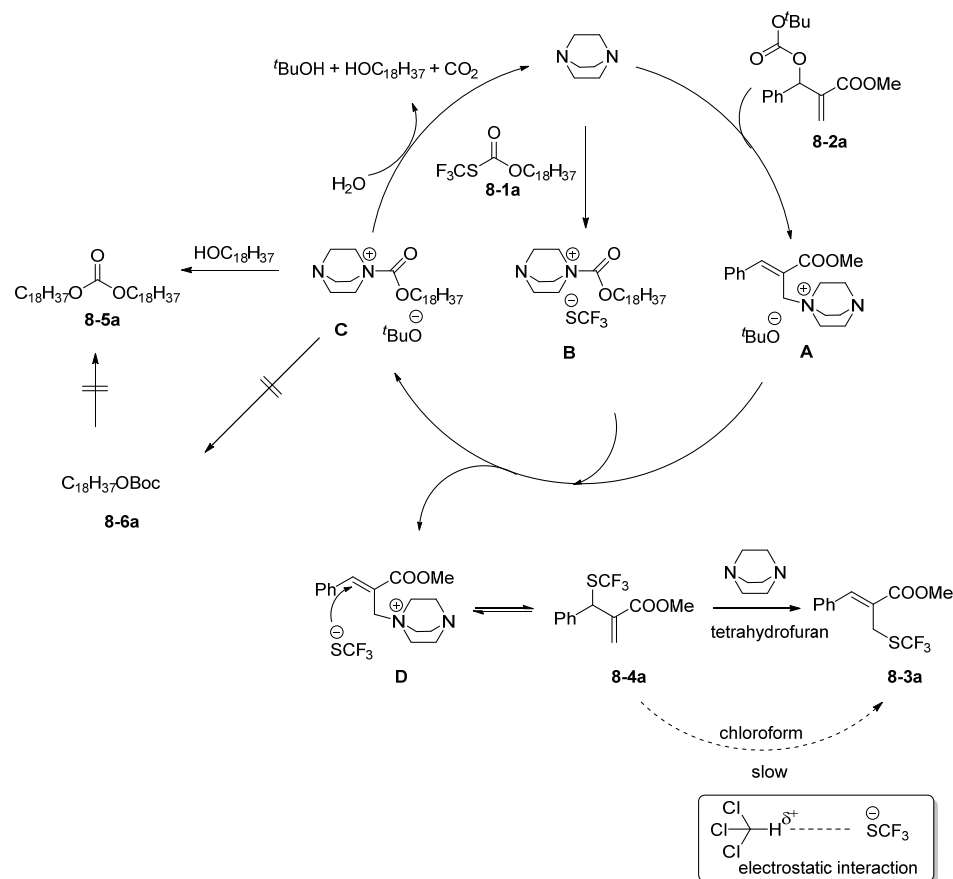
Shi and co-workers developed regioselective trifluoromethylthiolation between Morita–Baylis–Hillman (MBH) carbonates (**8-2**) and Zard's trifluoromethylthiolation reagent (**8-1a**) in the presence of DABCO (Scheme 16) [74]. A primary allylic trifluoromethylthiolate (SCF_3) was obtained as the favored product (**8-3**) when the authors used tetrahydrofuran as the solvent at room temperature, whereas when using chloroform at 0°C , this produced a secondary allylic trifluoromethylthiolate as a major product (**8-4**). The optimized reaction conditions with THF enabled the reaction to smoothly proceed with various MBH carbonates containing 4-Cl, 4-CN, 4-Br, and heterocyclic compounds such as 2-thienyl, 2-furyl, and 2-pyridyl to afford the primary allylic trifluoromethylthiolation products in good yields with good regioselectivities. Similarly, MBH carbonates containing 4-MeO, 3-Me, 4- NO_2 , and 2-pyridyl produced a secondary allylic trifluoromethylthiolate in the CHCl_3 solvent with good yields and high selectivities.



Scheme 16. Solvent-controlled nucleophilic trifluoromethylthiolation of MBH carbonates.

In the mechanism depicted in Scheme 17, this reaction proceeded with an initial nucleophilic addition of DABCO to **8-1a** and **8-2a**, forming the ammonium salt intermediates **A** and **B**, respectively. Then, the exchange of SCF_3^- and $^t\text{BuO}^-$ afforded the other intermediates **C** and **D**. The secondary allylic trifluoromethylthiolation product **8-4a** was obtained

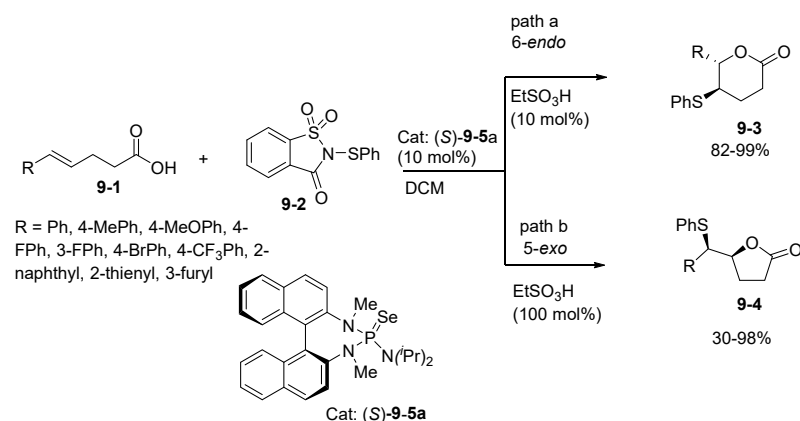
by an intermolecular S_N2' reaction of intermediate **D**. In the presence of the catalyst DABCO, the secondary product was readily converted to the primary product in THF, whereas the conversion in chloroform was difficult. This is attributed to electrostatic interaction between SCF_3^- and $CHCl_3$, weakening the nucleophilicity of the SCF_3^- anion. The catalyst DABCO was regenerated by the nucleophilic addition of water to intermediate **C**.



Scheme 17. Plausible reaction mechanism for trifluoromethylthiolation.

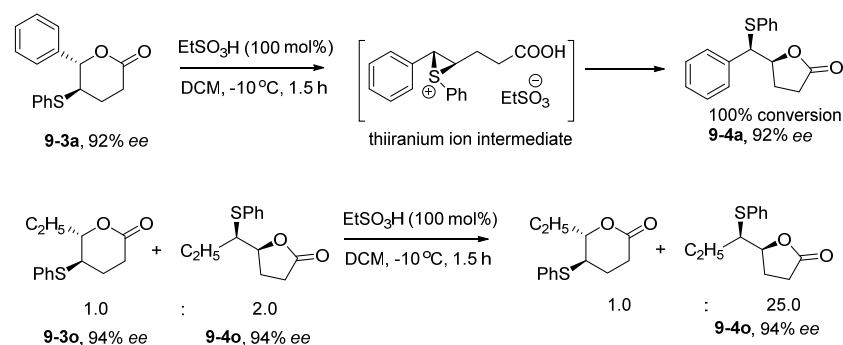
A divergent strategy was developed by Liu and Chen *et al.* for the modular synthesis of various enantioenriched phenylthio-substituted lactones from the thiolation of homoallylic acids via regiodivergent cyclization (Scheme 18) [75]. The authors developed Lewis base/Brønsted acid co-catalyst-controlled regio- and enantioselective thiolactonizations of a variety of homoallylic acid derivatives with different electrophilic SAr reagents (6-*endo* vs. 5-*exo*). The homoallylic acid (**9-1**) underwent 6-*endo* cyclization using *N*-phenyl thio-saccharin (**9-2**) as the sulfonylating agent, and chiral BINOL-derived selenide ((**S**)-**9-5a**) as the Lewis base. Various styrene-based carboxylic acids afforded the products (**9-3**) in excellent yields with high enantioselectivity, which was affected by the position of the substrate. For instance, a fluorine substituent in the *para* position resulted in high enantioselectivity compared with the *meta* or *ortho* positions. Moreover, 2-naphthyl, 2-thienyl, 3-furyl, and various substituted ethynylbenzenes underwent this reaction to afford δ -valerolactones in good yield with good enantioselectivity. In the presence of 1.0 equivalent of $EtSO_3H$ using *N*-phenylthiotphthalimide as the sulfonylating agent, and chiral BINOL-derived selenide as the Lewis base, homoallylic acids afforded various γ -butyrolactones (**9-4**). Styrene derivatives with various functional groups, irrespective of their position, underwent 5-*exo* cyclization to yield the corresponding five-membered ring products in good yields with high enantioselectivities. 2-Naphthyl and various unbiased alkyl-substituted alkenes proceeded smoothly to afford the products in good yields with high

enantioselectivities, whereas an ethynylbenzene-substituted alkene afforded the product in poor yield with moderate enantioselectivity.



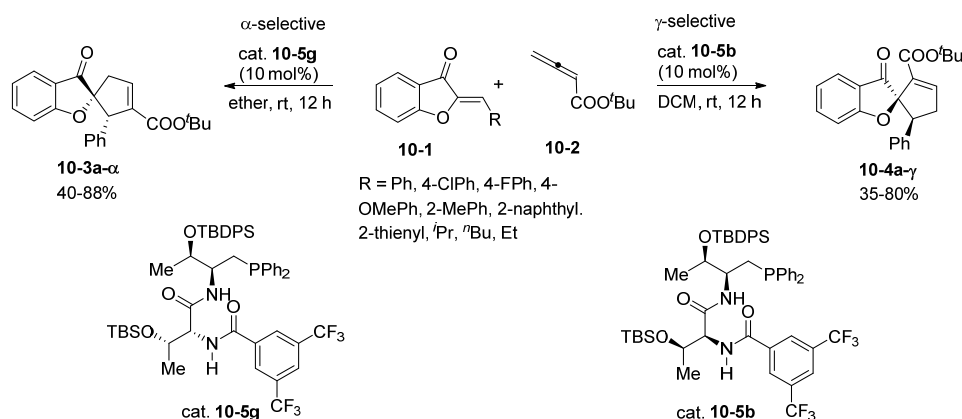
Scheme 18. Acid-controlled asymmetric thiolation of alkenes.

These researchers conducted experimental and computational studies to elucidate the origins of the regio- and enantioselectivity. The results of kinetic control experiments to acquire mechanistic information suggested that the 6-*endo* product (**9-3a**) could isomerize into a thermodynamic 5-*exo* product (**9-4a**) via the configurationally stable thiiranium intermediate under strongly acidic conditions (Scheme 19), which was further supported by the reaction between 6-*endo* and 5-*exo* with 100 mol% of EtSO₃H to afford a 5-*exo* product with retention of *ee*. The combination of DFT calculation results suggested that C-O and C-S bond formation might occur simultaneously, without formation of a commonly supposed catalyst-coordinated thiiranium ion intermediate. The potential π - π stacking between the substrate and SPh is an important factor in the enantio-determining step.



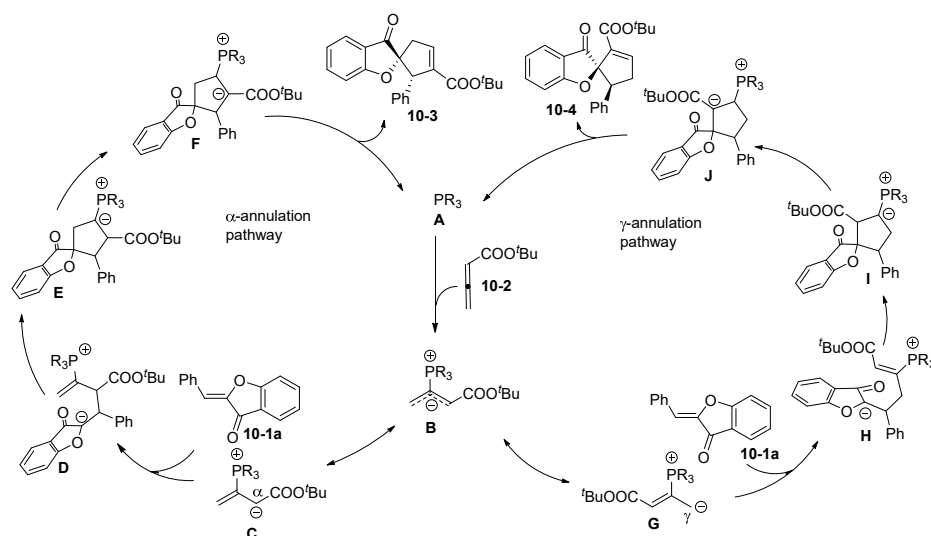
Scheme 19. Isomerization process under acidic conditions.

In 2017, Lu *et al.* developed the catalyst-controlled regioselective synthesis of spirocyclic benzofuranones via regiodivergent [3+2] annulations of aurones and allenates (Scheme 20) [76]. The use of the L-thr-D-thr-derived chiral phosphine catalyst **10-5g** in an ether in an annulation reaction produced the α -isomer **10-3** in moderate to good yield with excellent enantioselectivities. On the other hand, the L-thr-L-thr-derived chiral phosphine catalyst **10-5b** yielded the γ -isomer **10-4** in good yield with high enantioselectivities (96–99%). Under the optimized reaction conditions, various substituted aurones afforded α - or γ -selective spiro benzofuranones with excellent enantio- and regioselectivities depending on the catalyst present.



Scheme 20. Catalyst-controlled synthesis of spirocyclic benzofuranones.

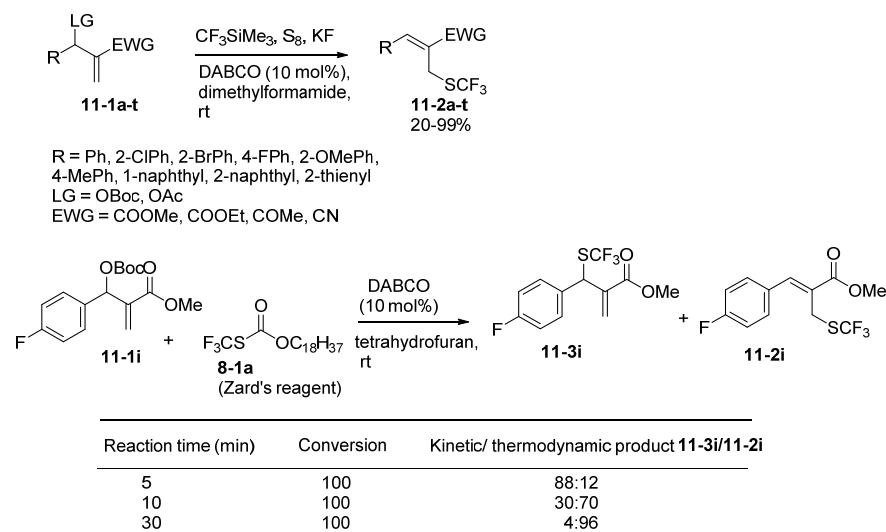
Mechanistic studies suggested that the phosphine catalyst attacked the allene (**10-2**) to form zwitterionic intermediate **B**, in which the negative charge may be delocalized either on the α -carbon or the γ -carbon (Scheme 21). Then, the aurone (**10-1a**) underwent [3+2] annulation with the putative intermediates, delivering intermediates **E** or **I**. Proton transfer followed by elimination of the phosphine catalyst furnished the α - and γ -selective products.



Scheme 21. Plausible mechanism for phosphine-catalyzed [3+2] annulation of aurones with allenoates.

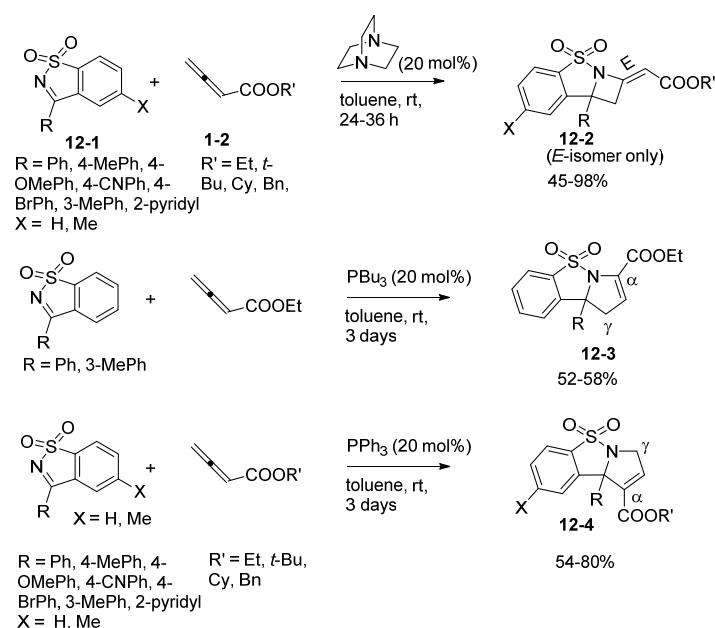
Cahard *et al.* reported the synthesis of primary and secondary allylic SCF₃ compounds in the presence of DABCO with Morita–Baylis–Hillman (MBH) carbonates (Scheme 22) [77]. The combination of CF₃SiMe₃/S₈/KF in DMF as the solvent afforded the primary product (**11-2**). Regardless of whether an EWG or EDG was present on the MBH carbonate, the primary allylic SCF₃ products formed in excellent yields. Sterically bulky groups such as 1- and 2- naphthyls and 2-thienyl were well tolerated in this trifluoromethyl thiolation reaction, furnishing the equivalent products in good yields. On the other hand, Zard's reagent (CF₃SCO₂C₁₈H₃₇) afforded the secondary allylic SCF₃ product (**11-3i**) when the reaction was conducted in the THF solvent at room temperature. The authors expected that the base DABCO would activate both Zard's reagent and the MBH carbonate and provide the secondary allylic trifluoromethyl thiolation product **11-3i** (kinetic

product) within 5 minutes. Upon extension of the reaction time to 30 min, the kinetic product (secondary) was rapidly isomerized into a thermodynamic product (**11-2i**, primary allylic trifluoromethyl thiolation product), as monitored by ^{19}F NMR.



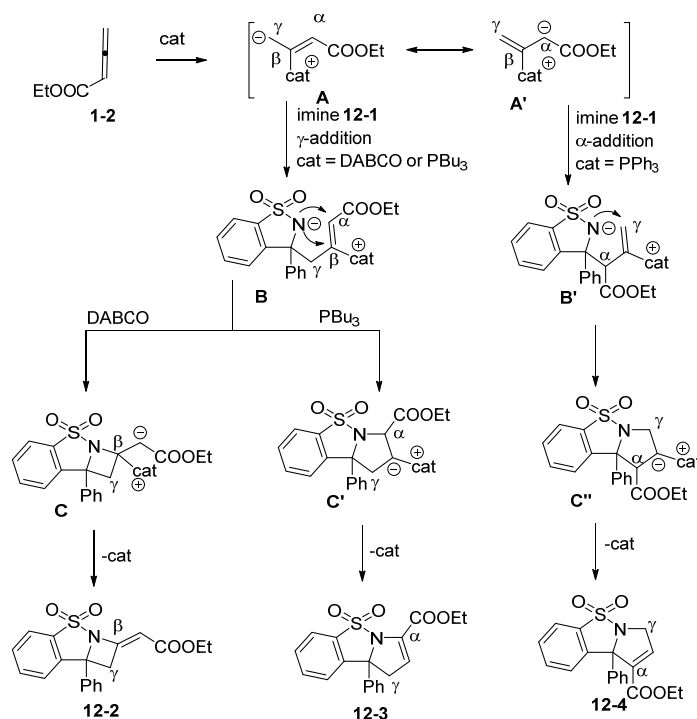
Scheme 22. Regio- and stereo-controlled nucleophilic trifluoromethylthiolation of MBH carbonates.

Ye's group established sultam-fused azetidines and dihydropyrroles via two different cycloadditions ([2+2] and [3+2]) from cyclic sulfonamide ketimines (**12-1**) and allenates (**1-2**). These compounds are formed by involving Lewis bases in the reaction (Scheme 23) [78]. In the toluene solvent at room temperature, PPh_3 , as a catalyst, underwent a [3+2] cycloaddition to produce **12-4** as the product via α -addition. The regioselectivity was switched in the case of PBu_3 , which led to a γ -cycloadduct (**12-3**). A completely different cycloaddition product was formed with the DABCO catalyst, delivering a [2+2] cycloadduct (**12-2**). Ketimines with an EDG or EDG worked well. Similarly, various allenates were also found to be suitable under optimized conditions.



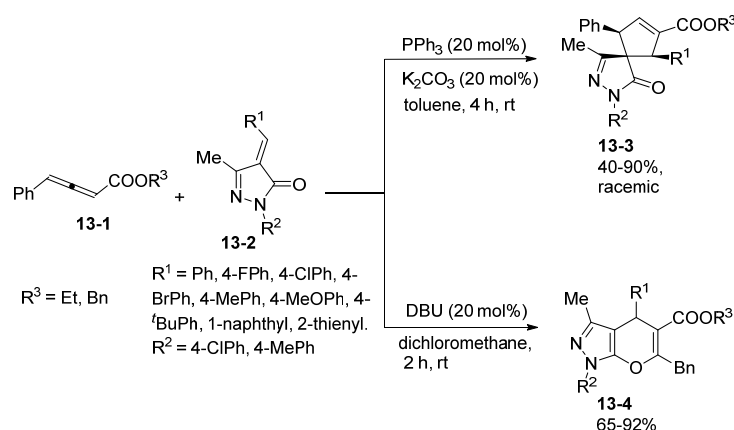
Scheme 23. Lewis base-catalyzed [2+2] and [3+2] cycloaddition reactions.

The authors also proposed a reaction mechanism (Scheme 24). They suggested that the reaction was initiated by adding Lewis bases to the allenolate (1-2) to generate two zwitterionic intermediates, **A** and **A'**, which react with the cyclicimines (12-1) to form intermediate **B** or **B'**. The carbanion **A'** was stabilized by the electron-poor nucleophile PPh_3 which then produced the thermodynamically favored α -addition intermediate **B'**, and elimination of the catalyst delivered 12-4. In the case of DABCO and PBU_3 , which are relatively electron-rich nucleophiles, they provided kinetically favored intermediate **B** via γ -addition. Later, these intermediates underwent ring closure, followed by the release of the catalysts, to afford the expected cycloaddition products (12-2 and 12-3).



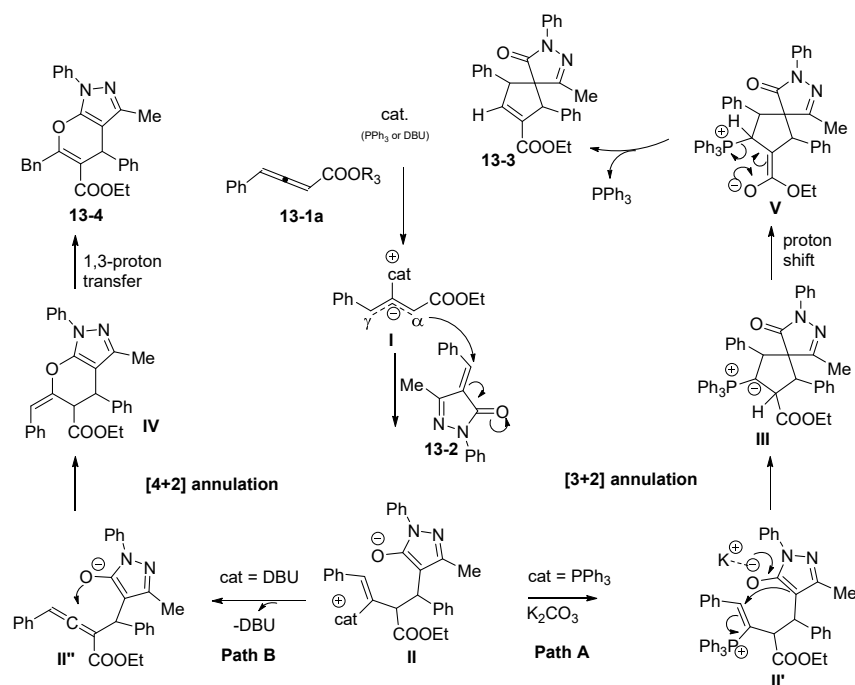
Scheme 24. Plausible catalytic cycles for cycloadditions.

Zhong and co-workers reported [3+2] annulation between γ -substituted allenolates (**13-1**) and unsaturated pyrazolones (**13-2**) to furnish spirocyclopentene-pyrazolones (**13-3**) when the reaction was performed in PPh_3 and K_2CO_3 (Scheme 25) [79]. In terms of the scope of the substrates, pyrazolones with an aryl ring bearing an EDG at the *para* position afforded higher yields than those bearing EWGs. Similarly, halogens such as Cl and Br, and 1- and 2-naphthalenes were compatible with the substrate to afford products. Allenolates containing *tert*-butyl instead of ethyl delivered spirocyclopentene-pyrazolones in lower yield owing to the steric hindrance.



Scheme 25. Lewis base-controlled [3+2] and [4+2] annulation reactions.

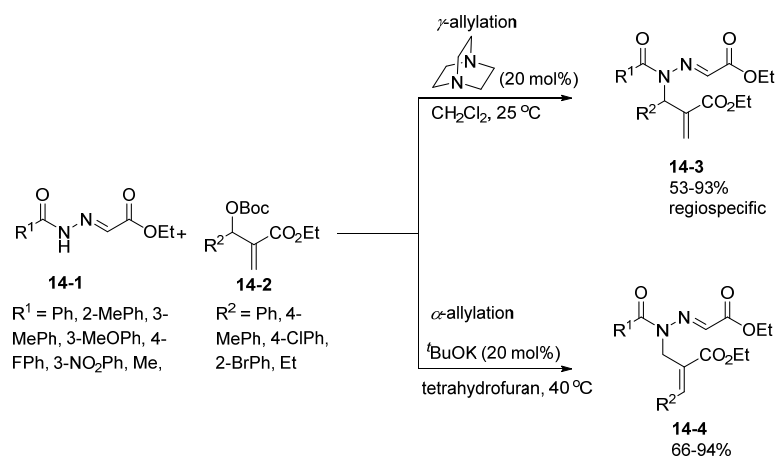
On the other hand, in the presence of DBU as a base, pyrano[2,3-*c*]pyrazoles (**13-4**) were obtained via [4+2] annulations. Pyrazolones containing F, Cl, Br, Me, *t*Bu, *i*Bu, 2-naphthyl, and 2-thienyl all reacted smoothly to afford pyrano[2,3-*c*]pyrazoles in good to excellent yields. With regard to the mechanism, the Lewis base catalyst attacks the allene to afford zwitterionic intermediate **I**, which then α -attacks the pyrazolones to form intermediate **II** via 1,4-addition (Scheme 26). The reaction can proceed along path **A**, in which case an intramolecular Michael addition takes place in the presence of PPh_3 and K_2CO_3 to afford intermediate **III**. Next, proton transfer and regeneration of the catalyst (PPh_3) furnish the [3+2] annulated product spirocyclopentene-pyrazolone (**13-3**). Path **B** involves elimination of the catalyst DBU to afford intermediate **II'** followed by an *O*-Michael addition to provide intermediate **IV**. Subsequently, 1,3-proton transfer of intermediate **IV** delivers the [4+2] annulated product pyrano[2,3-*c*]pyrazoles (**13-4**).



Scheme 26. Possible reaction mechanism for Lewis base-controlled annulation reactions.

In 2019, Sun *et al.* developed a regiodivergent allylation of *N*-acylhydrazones (NAHs, **14-1**) with Morita–Baylis–Hillman (MBH) carbonates (**14-2**), selectively affording α (**14-4**)–

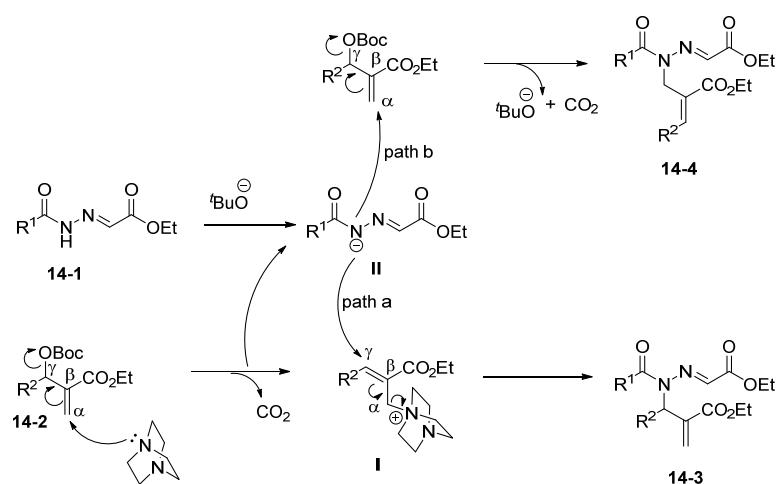
or γ (**14-3**)-allylated products (Scheme 27) [80]. The regioselectivity of the above methodology was precisely regulated by an expedient alternation of the catalysts to afford α - and γ -allylated *N*-acylhydrazone derivatives selectively in excellent yields.



Scheme 27. Proposed reaction pathways for base-promoted regiodivergent allylation.

The authors screened a wide range of base catalysts and identified $t\text{BuOK}$ and DABCO as the optimal catalysts to promote the formation of α - or γ -allylated products, respectively. In DABCO, the optimized conditions were compatible with a broad range of MBH carbonates having various EWGs and EDGs either at the *ortho* or *para* position of the phenyl ring and were tolerated. Similarly, NAHs having various functional groups in their aryl ring including Me, Cl, MeO, and F all afforded γ -allylated products (**14-3**) in good to excellent yields. On the other hand, due to the strong electron-withdrawing nature of the nitro group, it afforded the product, albeit in a lower yield. In a similar fashion, the substrate scope of $t\text{BuOK}$ -catalyzed α -allylation was explored (**14-4**). Various electron-donating and withdrawing groups were incorporated in both MBH carbonates and NAHs. The electronic effect or the bulkiness of the substituents did not affect the efficiency of the α -allylation, affording the products in good to excellent yields. However, an MBH carbonate derived from aliphatic aldehydes afforded the corresponding allylated product in the DABCO base, whereas this failed to occur in $t\text{BuOK}$.

In the proposed mechanism, the regiodivergent allylation proceeds through the key step involving deprotonation of *N*-Acylhydrazone (**14-1**) by $t\text{BuO}^-$ to produce nucleophilic intermediate **II** (Scheme 28). Intermediate **II** participates in the further reaction divergently in the presence of different catalysts to yield either α - or γ -allylated products. In path a, the attack of the DABCO catalyst on the α -position of the MBH carbonate (**14-2**) in an $\text{S}_\text{N}2$ fashion affords intermediate **I**. The $t\text{BuO}^-$ released in due course subsequently deprotonates **14-1**, leading to intermediate **II**. The key intermediate **II** reacts with intermediate **I** via the $\text{S}_\text{N}2$ pathway to produce the γ -allylated products (**14-3**). When $t\text{BuOK}$ is used as a catalyst, intermediate **II** approaches the α -position of **14-2**, leading to the α -allylated products (**14-4**) through the $\text{S}_\text{N}2$ pathway (path b).

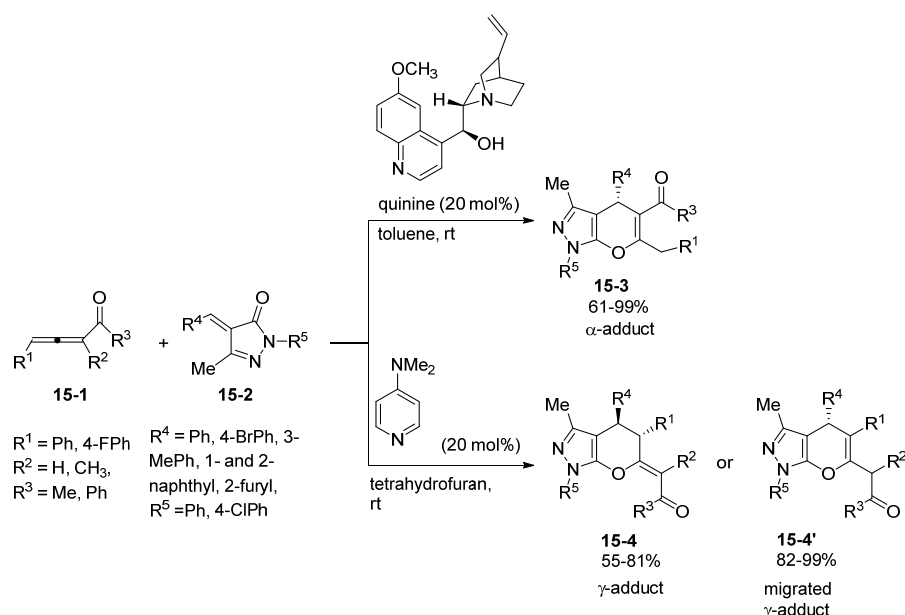


Scheme 28. Proposed reaction pathways for base-promoted regiodivergent allylation.

2.2. Cinchona Alkaloids

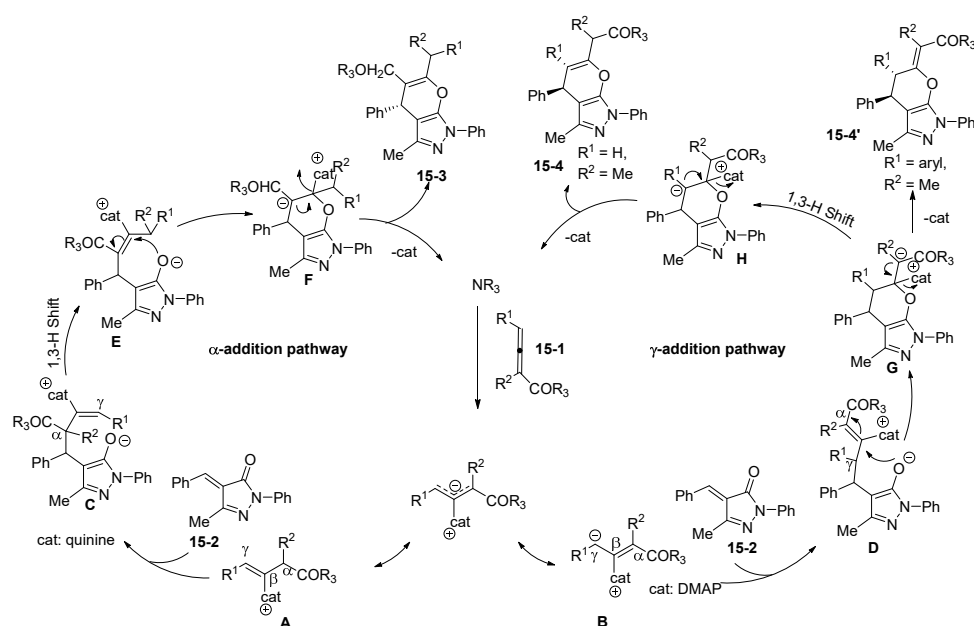
Both naturally occurring and modified cinchona alkaloids (quinine, quinidine, cinchonidine, cinchonine) are widely used in asymmetric synthesis. These alkaloids offer various important features such as numerous chiral centers, structural rigidity, multiple donors in the form of hydrogen bonds, and facile conversion into different functional groups including chiral quaternary ammonium salts [81–90]. Apart from this, they have various applications such as utilization in chiral ligands in the preparation of metal complexes, in NMR as chiral agents, resolving agents, chiral stationary phase in HPLC, electrolytic additives, and chiral solvating agents. They have been successfully used in various important asymmetric transformations such as the Mannich reaction [91–93], Michael addition [94–96], aza-Henry reactions [97,98], and epoxidation [99,100], in order to promote a highly enantio- and diastereoselective outcome.

Cheng *et al.* developed a Lewis base-catalyzed cycloaddition between allene ketones or α -methyl allene ketones and pyrazolones to produce tetrahydropyrano[2,3-*c*] pyrazoles in moderate to good yields via a [4+2] cycloaddition (Scheme 29) [101]. The annulation of benzylidenepyrazolones (15-2) with allene ketones (15-1) proceeded smoothly via either an α - or γ -selective pathway, and the desired products were obtained in good yields with high regioselectivities. The use of quinine as the catalyst favored the formation of an α -adduct (15-3) with high regioselectivity in a 99% yield. After optimizing the conditions, the authors examined various substrates (neutral groups, EWGs, and EDGs as substituents at the *ortho*, *meta*, or *para* position on benzylidene pyrazolones) and found that they are capable of delivering the expected products in good yields with excellent regioselectivities. Interestingly, pyrazolone containing α -naphthyl, β -naphthyl, and 2-furyl groups reacted smoothly and furnished the anticipated product in good yield with high regioselectivity. On the other hand, DMAP produced the γ -selective cycloaddition products as the major regioisomers in good yield (15-4). This γ -selective [4+2] annulation of various substrates with DMAP was then investigated. Pyrazolone with α -naphthyl-, β -naphthyl-, 2-thienyl-, and 2-furyl-containing substrates efficiently reacted under the standard conditions to produce the expected products in good yield with high regioselectivity.



Scheme 29. Lewis base-catalyzed regioselective [4+2] cycloaddition.

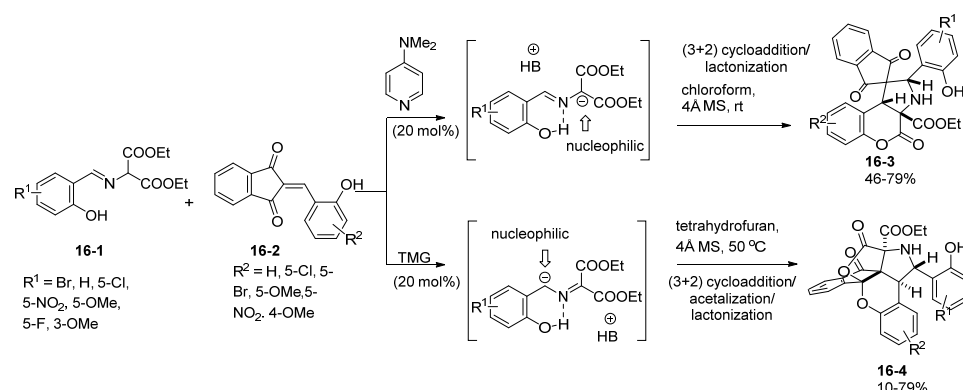
According to the proposed reaction mechanism (Scheme 30), first, the Lewis bases undergo addition with the allene ketones (**15-1**) to generate zwitterionic intermediates, which then undergo nucleophilic addition with the unsaturated pyrazolones (**15-2**) to form intermediates **C** and **D** via α- or γ-addition. An electron-poor nucleophile such as quinine may stabilize carbanion **A** and lead to a thermodynamically feasible α-addition, whereas a kinetically favored γ-addition could occur at carbanion **B** in the case of the electron-rich nucleophile DMAP. Further, a proton shift and subsequent ring closure of the intermediates via an oxygen anion or in reverse mode would then generate the cyclic adducts **F** and **H**, respectively. These adducts result in the formation of regiodivergent products after elimination of the Lewis bases from the cyclic adducts.



Scheme 30. Proposed reaction mechanism of cycloaddition catalyzed by Lewis bases.

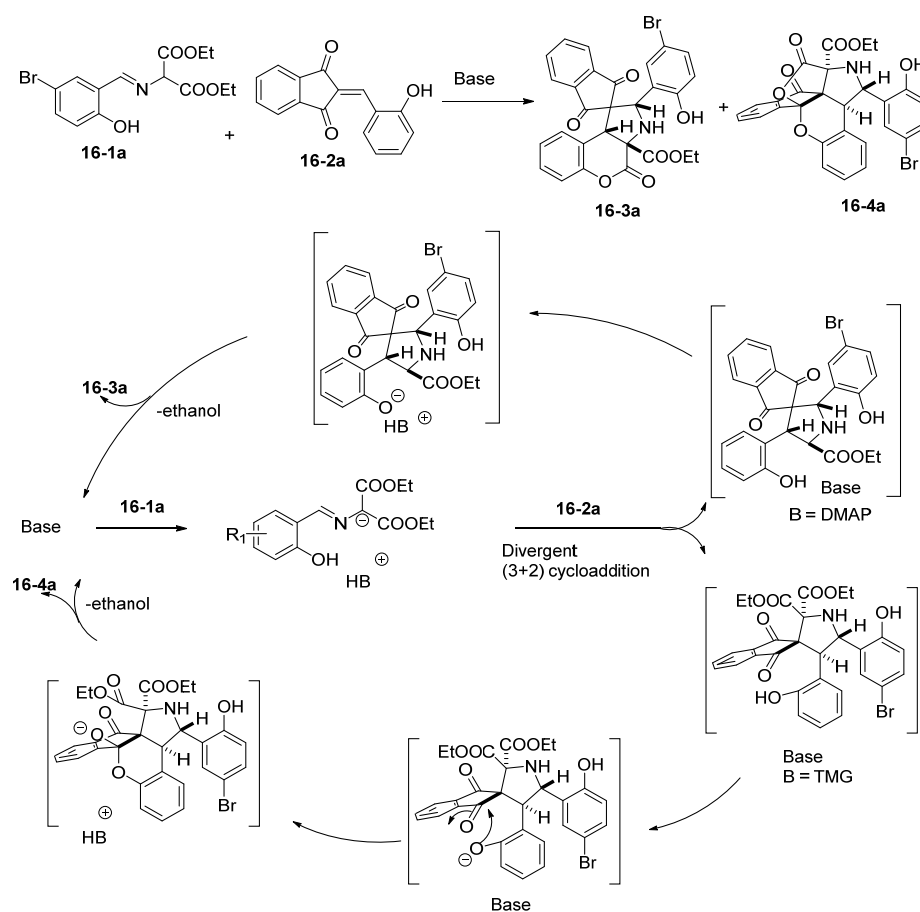
A regiodivergent 1,3-dipolar cycloaddition of azomethine ylides (**16-1**) and 2-hydroxybenzylidene indandiones (**16-2**) was developed by Lin *et al.* in 2018 (Scheme 31)

[102]. The (3+2) cycloaddition, which involved the reversal of the nucleophilic site in azomethine ylides, was controlled by choosing suitable base catalysts, DMAP and 1,1,3,3-tetramethylguanidine (TMG), which subsequently resulted in two different cascade processes to generate the diverse chromenopyrrolidines **16-3** and **16-4**, respectively. The azomethine ylide was stabilized by the conjugate acids of the bases in two different conformations via hydrogen bonding, which afforded regiodivergent (3+2) cycloadditions. Subsequent cyclization delivered the above products in moderate to good yields (as high as 84%) and with excellent diastereo- and enantioselectivity (as high as 96%).



Scheme 31. Base-controlled regiodivergent [3+2] cycloaddition.

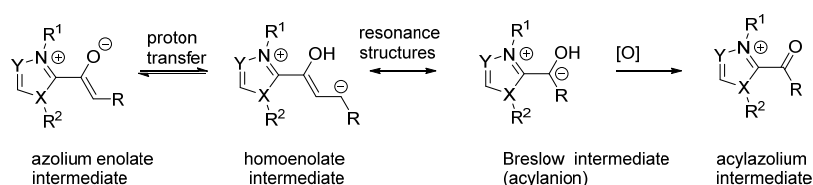
According to the plausible mechanistic pathway (Scheme 32), initially, the iminodiester (**16-1a**) is deprotonated in the presence of bases to form the equivalent conjugate acids, which then subsequently participate in hydrogen bonding with the azomethine ylide. The use of the electrophile 2-hydroxybenzylidene indan-1,3-dione (**16-2a**) introduces steric hindrance and leads to two different transition states. In the presence of DMAP as the base, a [3+2] cycloaddition followed by cascade lactonization affords the expected product, chromeno[3,4-*b*]pyrrolidines (**16-3a**). The unanticipated chromeno[3,4-*c*]pyrrolidine adduct **16-4a** is obtained when TMG is used as the base. This is the consequence of the opposite regioselectivity during the initial (3+2) cycloaddition, subsequent acetalization, and lactonization. Both the regiodivergent adducts **16-3a** and **16-4a** were further confirmed by X-ray diffraction analysis. The steric hindrance on the azomethine ylide resulting from TMG exceeded that introduced by DMAP, which led to the regioselective reversal in the (3+2) cycloaddition. The control experiments and NMR studies of the deprotonation of the iminodiester (**16-1**) by DMAP and TMG were in alignment with the proposed mechanism.



Scheme 32. Possible reaction mechanism for base-controlled regiodivergent [3+2] cycloaddition.

2.3. NHC Catalysts

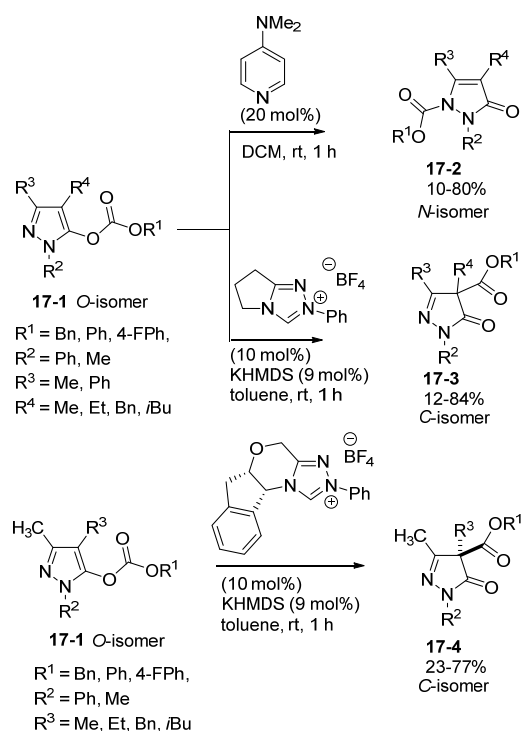
The widespread use of NHC has revealed it to be an important organocatalyst that has been used in many synthetic strategies. Catalysts based on NHC are widely utilized for the synthesis of various biologically important natural products as well as pharmaceutical drugs [31]. Usually, these catalysts are used in C-C and C-heteroatom bond formation reactions and involve various cycloaddition reactions such as [2+2], [2+2+2], and [2+4]. These cycloadditions are generally achieved by the catalytic ability of NHC, which alters the polarity of a carbonyl compound via NHC-linked intermediates such as the Breslow, azolium enolate, acylazolium, and homoenolate intermediates (Scheme 33) [103–113].



Scheme 33. NHC-linked intermediates.

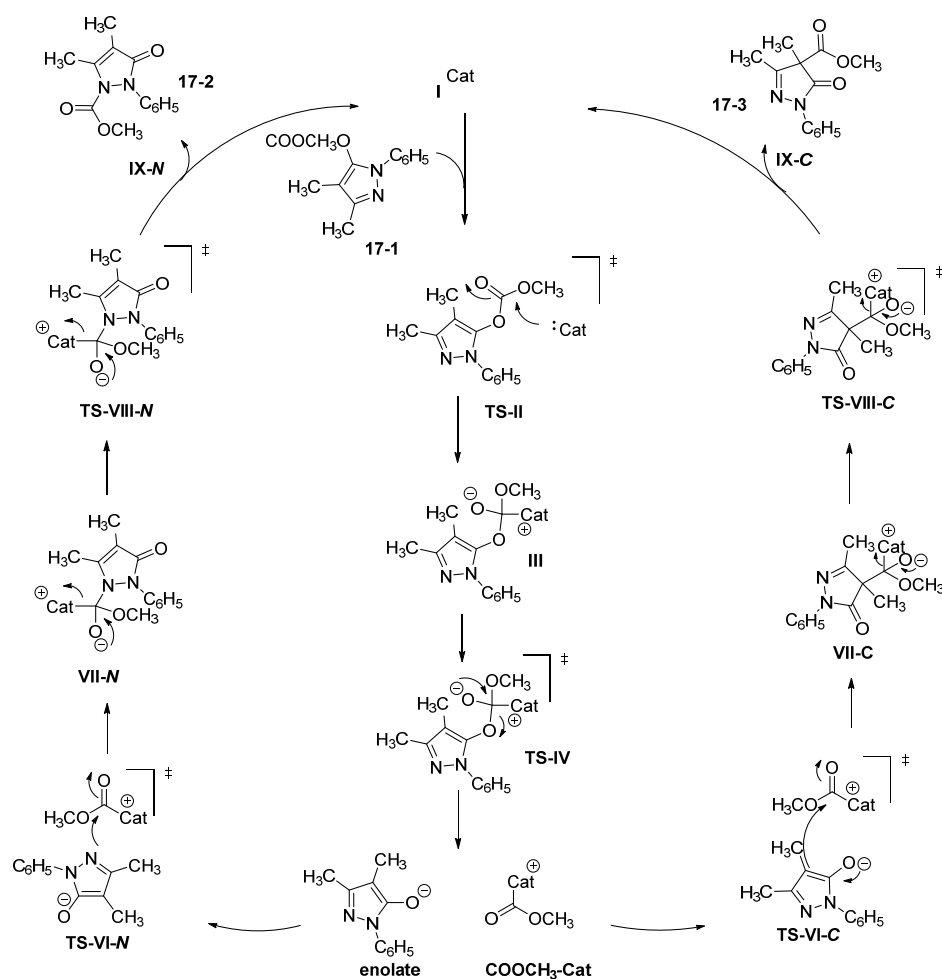
In 2014, Smith and co-workers described a regiodivergent O- to C- or N-carboxyl transfer of pyrazolyl carbonates (17-1) by the choice of catalyst (Scheme 34) [114]. Specifically, DMAP in dichloromethane delivered kinetically favored O- to N-carboxyl transfer with good regioselectivity (as high as 99%) and low to good yields (17-2, 10–80%), whereas triazolinyldene NHC in toluene afforded thermodynamically favored O- to C-carboxyl transfer with good regioselectivity (as much as 99%) and low to good yields (17-3, 12–84%). In addition to that, the chiral triazolium NHC catalyst promoted enantioselective

(as high as 92%) and regioselective (as high as 99%) *O*- to *C*-carboxyl transfer products in good to excellent yields (**17-4**).



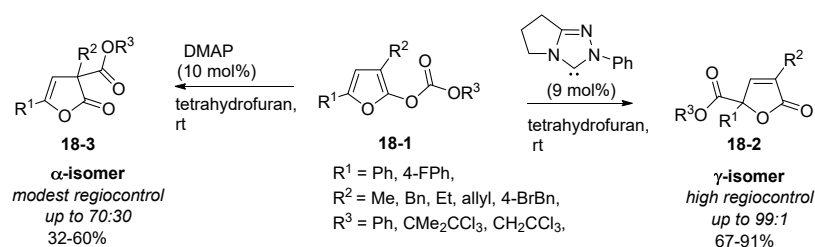
Scheme 34. Selective regiodivergent *O*- to *C*- or *N*-carboxyl transfer of pyrazolyl carbonates catalyzed by Lewis bases.

Further mechanistic experiments led to the conclusion that *O*- to *C*- or *N*-carboxyl transfer in pyrazolyl carbonates with DMAP was irreversible because the formation of the *N*-carboxylation product is kinetically favored. Contrary to this, *N*- to *C*-carboxyl transfer is not possible with DMAP. The *O*- to *C*- or *N*-carboxyl transfer with triazolinyldene NHCs is reversible because the formation of the *C*-carboxylation product is thermodynamically favored, and *N*- to *C*-carboxyl transfer is also considered to be feasible. On the other hand, *O*- to *C*- or *N*-carboxyl transfer is irreversible, with the chiral NHC catalyst exercising good enantiocontrol, although *N*- to *C*-carboxyl transfer is allowed with high enantiocontrol. Further, DFT studies supported the proposed mechanistic pathway shown in Scheme 35. Initially, the catalyst attacks the *O*-carboxylate to form the tetrahedral intermediate **TS(IV)**. Then, consecutive collapse of **TS(IV)** produces two common intermediates, enolate and a carboxylated catalyst, after which the carboxylated catalyst could be recaptured by the enolate either at *C*(4) or *N*(1) to produce (**TS-VII**). Finally, regeneration of the catalyst from the tetrahedral intermediate (**TS-VIII**) affords the two regiodivergent products (**17-2**, **17-3**).



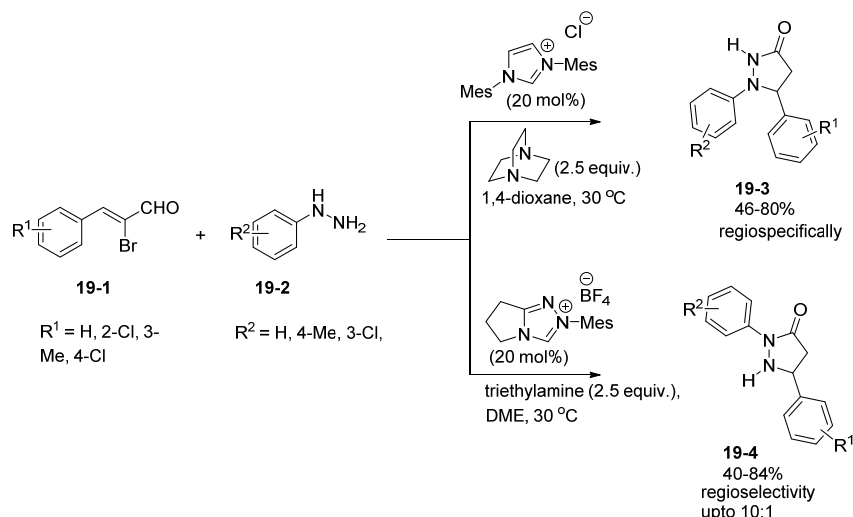
Scheme 35. Proposed reaction mechanism for O- to C- and N-carboxylation.

In 2015, Smith *et al.* reported regioselective carboxylation either at the γ - or α -position depending on the Lewis base involved (Scheme 36) [115]. Treatment of a furanyl carbonate (**18-1**) with the triazolinyldene NHC catalyst produced a γ -isomer with regioselectivity as high as 99:1 (**18-2**). Under optimal conditions, phenyl, trichloro ethyl, and certain sterically hindered substrates were well tolerated to afford the corresponding γ -C(5) carboxylation product in good to high yields. In contrast, the α -isomer product was generated by changing the catalyst to DMAP with moderate regiocontrol (60:40) to produce the α -C(3)-carboxylate as the major product (**18-3**). Individual treatment of the α - and γ -isomers with DMAP did not result in transformation, and the starting material was recovered even though the reaction time was prolonged. The α -carboxyl product underwent regioisomeric exchange in the presence of the NHC catalyst to afford the α/γ products in a 16:84 ratio, with the γ derivative as the major product. Similar results were obtained when the γ -regioisomer was reacted in the presence of the NHC catalyst to afford a 14:86 ratio of α/γ . These results revealed that C-carboxylation with DMAP is irreversible to preferentially yield the α -regioisomer. However, in the case of the NHC catalyst, C-carboxylation resulted in the formation of the γ -isomer as the major product followed by subsequent equilibration to form a mixture of α/γ products.



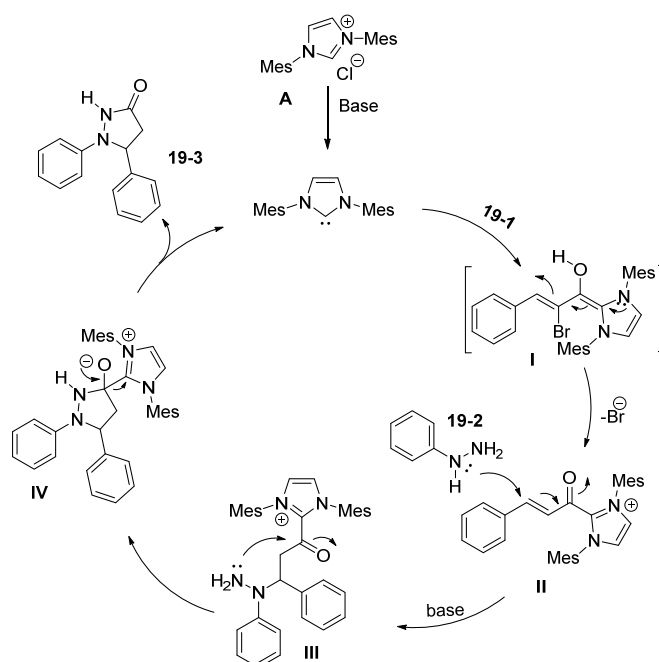
Scheme 36. Lewis base-promoted O- to C-carboxyl transfer of furanyl carbonates.

Yao *et al.* demonstrated the regioselective synthesis of 3-pyrazolidinones via NHC-catalyzed [3+2] annulation of α -bromoaldehydes (**19-1**) with hydrazine (**19-2**) in the presence of a base (Scheme 37) [116]. A regioselective methodology was devised by carefully adjusting the NHC catalysts, i.e., the imidazolium NHC precursor produced the 1,5-disubstituted 3-pyrazolidinone (**19-3**), whereas the triazolium NHC precatalyst was able to drive the reaction to completion to furnish the 2,5-difunctionalized isomer (**19-4**). Specifically, the regioselective Michael addition of the key intermediate to phenylhydrazine followed by subsequent lactamization afforded the regiodivergent products (**19-3**, **19-4**). This protocol was an attractive strategy for the assembly of biologically significant 3-pyrazolidinones in moderate to high yields (as high as 84%), under mild reaction conditions, and with good regioselectivity.



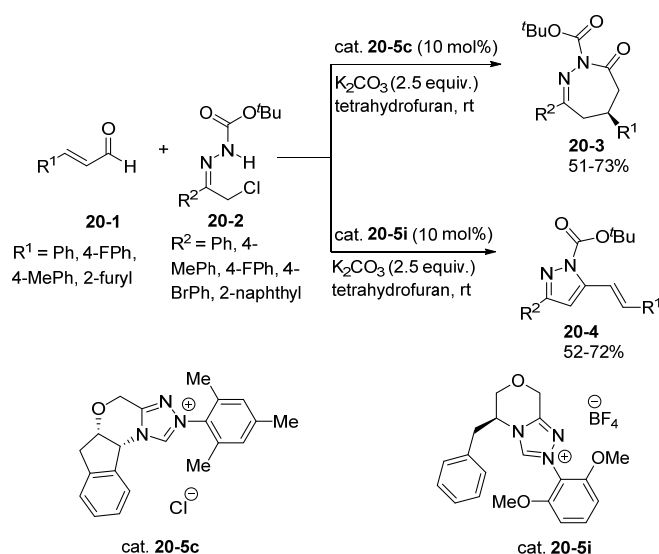
Scheme 37. NHC-catalyzed regiodivergent synthesis of 3-pyrazolidinones.

The authors proposed a plausible mechanistic pathway to explain the formation of product **19-3** (Scheme 38). Initially, the addition of the NHC catalyst to the α -bromoaldehyde forms the Breslow intermediate **I**, which is further debrominated into the α,β -unsaturated acylazolium intermediate **II** followed by Michael addition with phenylhydrazine, producing intermediate **III**. This intermediate then undergoes lactamization to afford the target compound **19-3** and the regenerated catalyst. Although the origin of the regioselectivity aided by the tuning of the catalyst remains uncertain, the authors suggested that a computational study on the relationship between the structure of the catalysts and the regioselectivities would aid further understanding.



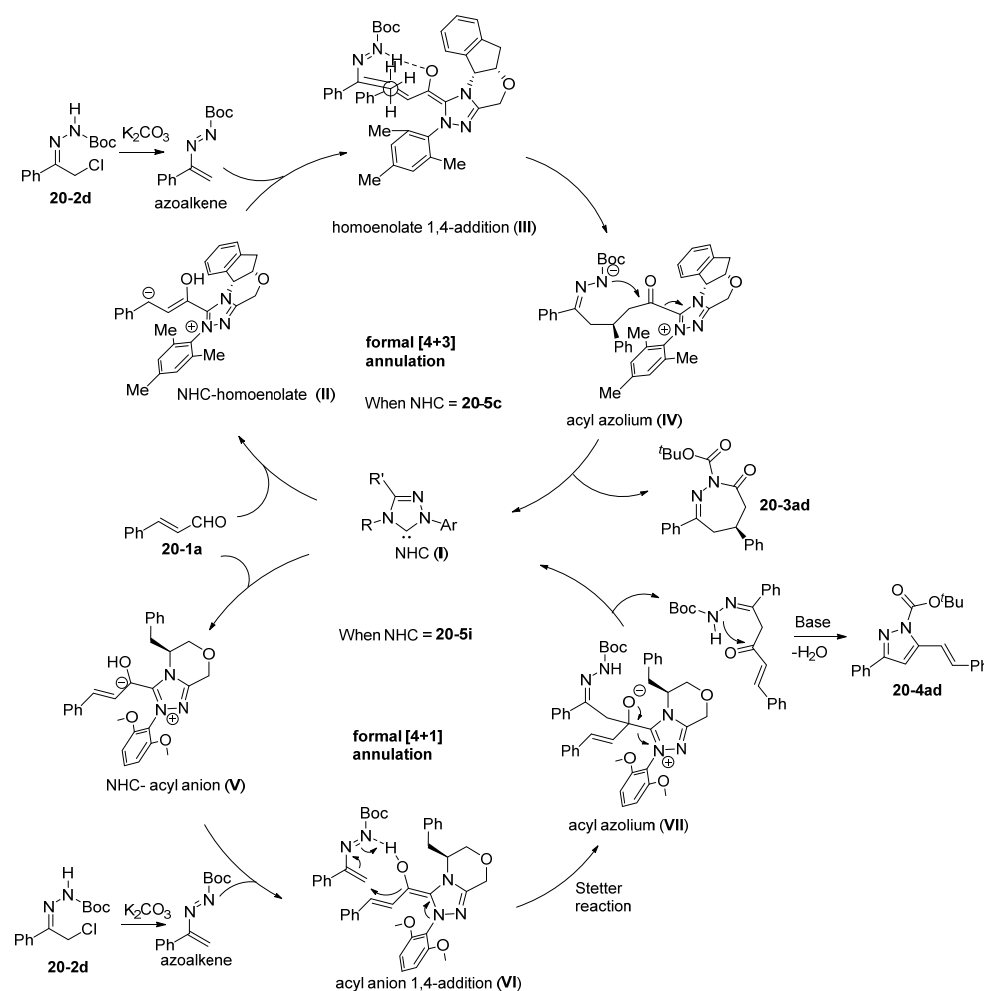
Scheme 38. Proposed catalytic cycle for the synthesis of 3-pyrazolidinones.

Glorius *et al.* devised a scheme for the synthesis of 1,2-diazepines (**20-3**) via formal [4+3] annulation and the synthesis of pyrazoles (**20-4**) via formal [4+1] annulation reactions along highly regio- and enantioselective pathways (Scheme 39) [117]. The reaction between enals (**20-1**) and hydrazones (**20-2**) in the presence of the chiral triazolium NHC catalyst **20-5c** afforded 1,2-diazepine derivatives through the homoenolate intermediate along a [4+3] annulation pathway. Various substituted enals containing both an EWG and EDG on the aromatic ring afforded the expected diazepine products in good yields with excellent enantioselectivities (99% *ee*). Similarly, hydrazones with different substituents reacted with enals via formal [4+3] annulation to form 1,2-diazepines in high yields with excellent enantioselectivities (99% *ee*). The use of the NHC catalyst with a morpholine backbone (**20-5i**) afforded the pyrazole derivatives with high regioselectivity (<1:20) via a Stetter reaction and subsequent cyclization reaction. This reaction occurred though the acyl anion intermediate initiated by the **20-5i** NHC catalyst which suppressed the homoenolate reactivity of enals to produce the pyrazoles.



Scheme 39. NHC-catalyzed formal [4+3] and [4+1] annulations for the synthesis of 1,2-diazepines and pyrazoles.

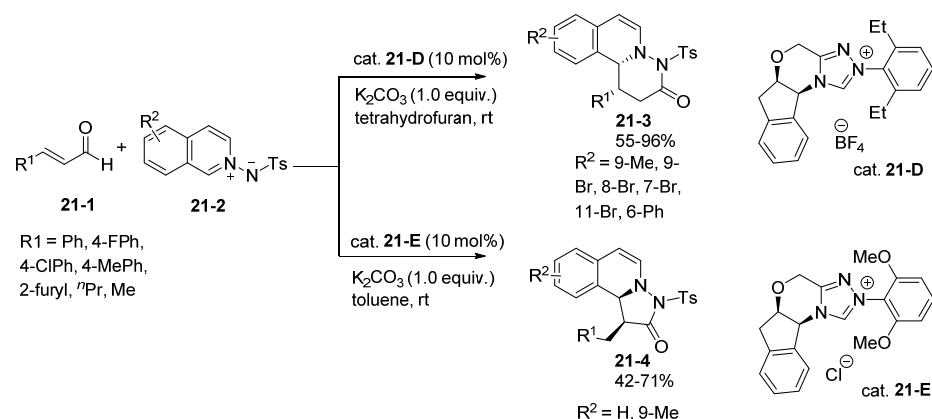
According to the proposed reaction mechanism (Scheme 40), the chiral NHC catalyst initially undergoes addition to the enal cinnamaldehyde (**20-1**) to form two Breslow intermediates (**II** and **V**). The structure of the NHC is suggested to play a crucial role in determining the reaction pathways to form either a haloenolate or acyl anion. Specifically, *N*-Mes containing NHC catalyst **20-5c** preferentially forms a homoenolate intermediate (**II**), whereas the reaction pathway via the acyl anion (**V**) predominantly occurs with the NHC-based catalyst *N*-2,6-(OMe)₂ (NHC **20-5i**). Then, the homoenolate intermediate **II** undergoes conjugate addition with the in situ formed azoalkene, followed by C-C bond formation. Subsequent *N*-acylation delivers [4+3] annulated product 1,2-diazepine (**20-3**) after regeneration of the NHC catalyst **20-5c**. On the other hand, the NHC **20-5i**-bound acyl anion intermediate **V** undergoes a Stetter reaction with the in situ generated azoalkene to afford adduct **VII**. The release of NHC **20-5i** followed by intramolecular cyclization and dehydration affords the final [4+1] annulation pyrazole product (**20-4**).



Scheme 40. Proposed catalytic cycle for the synthesis of 1,2-diazepines and pyrazoles.

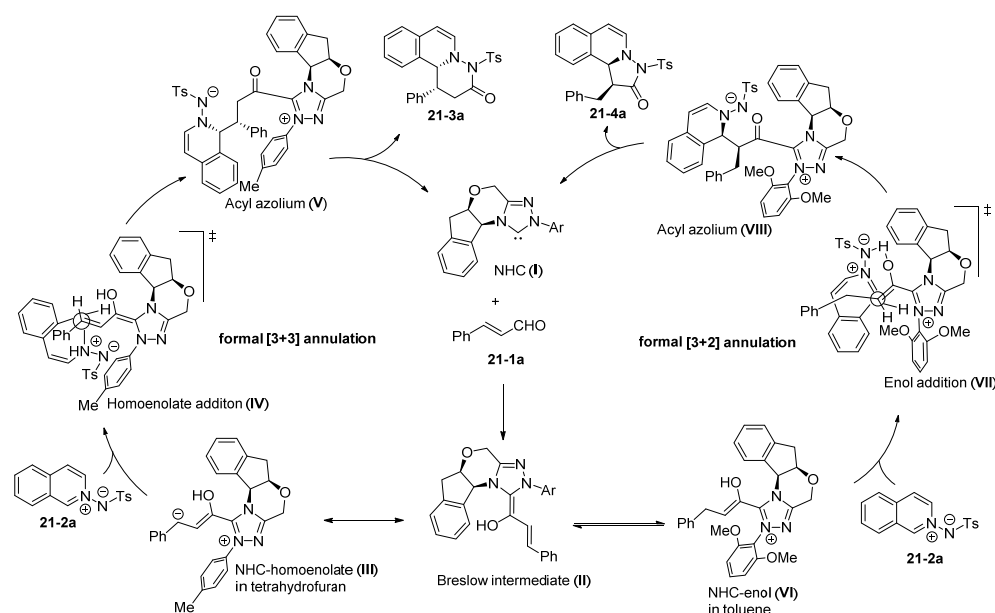
Glorius and co-workers also reported the NHC-catalyzed regiodivergent synthesis of pyridazino[6,1-*a*]isoquinoline and pyrazolo[5,1-*a*]isoquinolines by formal [3+3] and [3+2] annulations via a homoenolate intermediate and an enol intermediate, respectively (Scheme 41) [118]. The reaction between enals (**21-1**) and *N*-iminoisoquinolinium ylides (**21-2**) produced the above products in good to high yields with high enantiomeric excess. The formation of regiodivergent products was governed by the NHC precatalyst, base,

and solvent of the reaction. Initially, the homoenolate intermediate formed by the reaction between α,β -unsaturated aldehydes and the NHC catalyst was converted into an enol intermediate by subsequent protonation at the β -position. The conjugate acid of the catalytic base was generated from the azolium salt by deprotonation, depending on whether this was sufficiently acidic to protonate the homoenolate, to afford the [3+2] annulation product via the formation of the enol intermediate. The authors also concluded that the addition of a base (DBU) would limit the formation of the enol intermediate, whereas increasing the proton concentration by the addition of an acid (acetic acid) would produce a greater amount of **21-4** by promoting the formation of the enol intermediate. The optimized conditions were compatible with various enals and *N*-iminoisoquinolinium ylides containing both an EWG and EDG, which reacted to produce the formal [3+3] annulated products in good yield with high *ee* when the **21-D** NHC catalyst was employed. In the presence of NHC catalyst **21-E**, formation of the NHC-enolate intermediates was predominant to afford the pyrazolo[5,1-*a*]isoquinoline product via formal [3+2] annulation by suppressing the homoenolate intermediate. Under the optimized conditions, various enals and *N*-imino-3-phenylisoquinolinium ylides delivered the expected products in good yields with excellent *ee* and *dr* (20:1).



Scheme 41. NHC-catalyzed regiodivergent dearomatizing annulation reaction.

In the proposed reaction mechanism (Scheme 42), addition of the NHC precatalyst to the α,β -unsaturated aldehydes (**21-1**) produces the common Breslow intermediate **II**. Under strongly basic conditions, the Breslow intermediate reacts with *N*-iminoisoquinolinium ylide (**21-2**) to afford the acyl azolium **V** intermediate via a homoenolate intermediate. Regeneration of the catalyst from the acyl azolium affords the [3+3] annulated product (**21-3**). On the other hand, the Breslow intermediate undergoes β -protonation to form the enol equivalent **VI** under weakly basic reaction conditions. The subsequent addition of intermediate **VI** forms the acyl azolium **VIII** intermediate, which, on *N*-acylation, delivers the formal [3+2] annulated product (**21-4**) followed by regeneration of the NHC precatalyst.



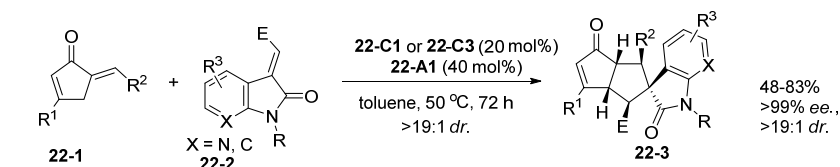
Scheme 42. Proposed reaction mechanism for NHC-catalyzed switchable annulation reaction.

3. Amine Catalysts

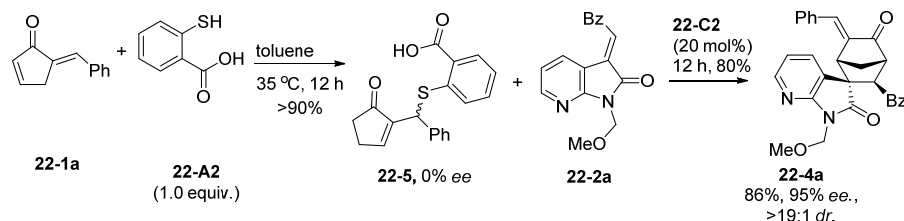
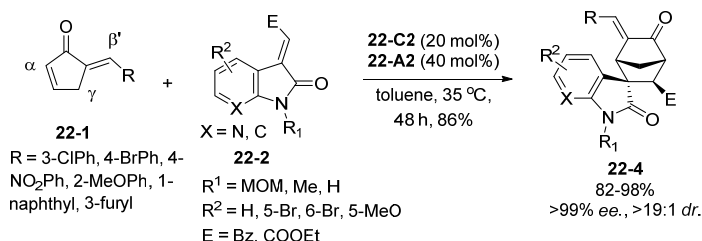
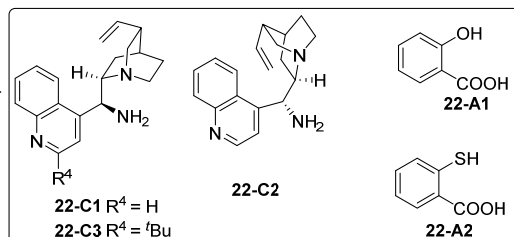
In the past two decades, L-proline and its derivatives have found rapidly growing application in various transformations to yield products with excellent *ee* and *dr* [119–126]. Remarkable advances have been made after the seminal work of List [127,128], Córdova [129,130], Barbas [131,132], and many other research groups. The discovery that a simple and effective catalyst such as L-proline could be put to effective use was a landmark achievement in this century and opened a new avenue for asymmetric synthesis. Despite the development of several modified proline catalysts, proline is still placed at the top of the list in terms of its performance. An enormous number of chemical transformations have been conducted by using derivatives of chiral organocatalysts including Aldol, Mannich, Michael addition, and Diels–Alder reaction, and if required, these catalysts are able to induce remarkable stereoselectivity. Importantly, several natural products and drugs have been synthesized by using these L-proline-derived catalysts [133–142].

Chen *et al.* disclosed switchable intermolecular regioselective [6+2] and [4+2] cycloadditions of α' -benzylidene-2-cyclopentenones with activated alkenes in the presence of a chiral primary amine catalyst and co-catalyst in high yields with high enantioselectivity (Scheme 43) [143]. The asymmetric intermolecular γ , β' -regioselective [6+2] cycloaddition of α' -benzylidene-2-cyclopentenones (**22-1**) with 3-olefinic 7-azaoxindoles (**22-2**), driven by the catalytic activity of the **22-C1** or **22-C3** chiral amine, with salicylic acid (**A1**) as the co-catalyst, provided thermodynamically stable fused bicyclic compounds with five contiguous stereogenic centers in toluene with excellent enantioselectivities (**22-3**). The cycloaddition proceeds through the in situ generated formal 4-amino fulvene, which served as a 6 π partner. Interestingly, the cycloaddition in the presence of the chiral amine **22-C2** and co-catalyst 2-mercapto benzoic acid (**22-A2**) switched to an α , γ -regioselective [4+2] cycloaddition with the generation of a dienamine intermediate which reacted with the alkene to afford bridged bicyclo[2.2.1]heptane derivatives (**22-4**). The proposed mechanism (Scheme 44) whereby these cycloadditions occur involves the formation of an imine intermediate with α' -benzylidene-2-cyclopentenones (**22-1**) with the aid of the chiral primary amine catalyst **22-C1**. This iminium intermediate is then converted into a 4-aminofulvene (cross-conjugated trienamine) intermediate. Then, a [6+2] cycloaddition with an alkene affords the bicyclic γ , β' -regioselective product **22-3** by the elimination of the chiral amine catalyst **22-C1**. For the [4+2] cycloaddition reaction, initially, β' -regioselective sulfur addition takes place with the benzylidene-2-cyclopentenones, which then under-

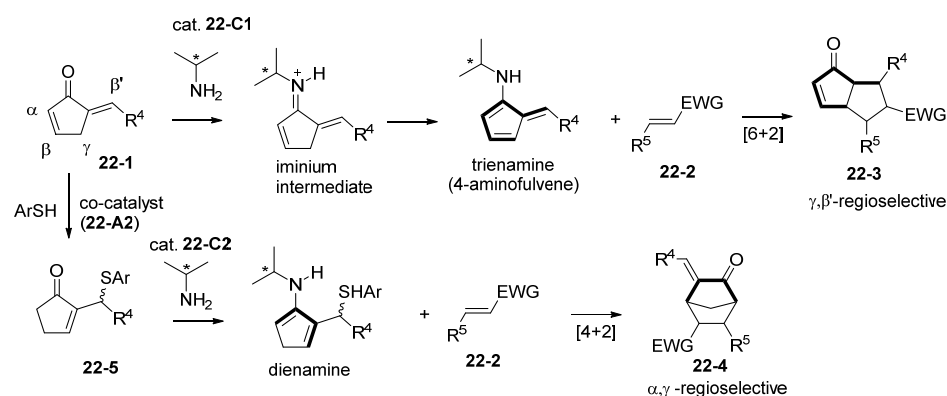
goes C=C bond isomerization to produce an enone with a sulfide intermediate (**22-5**). Addition of the amine catalyst and alkene to intermediate **22-5** forms the corresponding product (**22-4**) via a dienamine-mediated [4+2] cycloaddition, followed by the elimination of mercaptobenzoic acid (**22-A2**).



$R = \text{MOM, Me, H,}$
 $R^1 = \text{Me, Ph}$
 $R^2 = 3\text{-ClPh, 4-BrPh, 4-CNPh, 4-NO}_2\text{Ph, 1-naphthyl, 2-thienyl, 2-furyl, 2-styryl, }^i\text{Pr, }^t\text{Pr}$
 $R^3 = \text{H, Cl, Br}$
 $E = 4\text{-MeBz, 4-CF}_3\text{Bz, CN}$



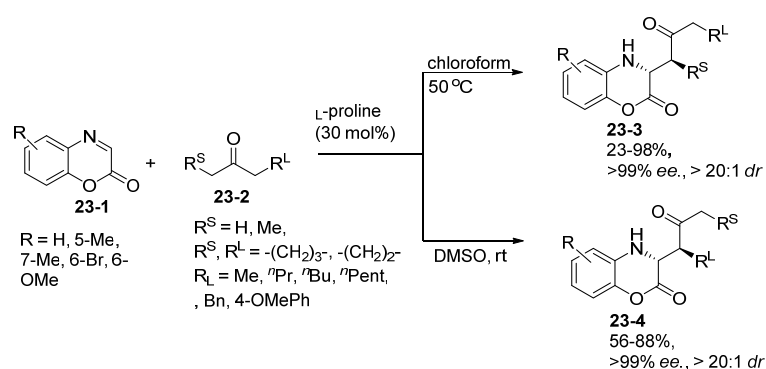
Scheme 43. Chiral amine-catalyzed [6+2] and [4+2] cycloaddition reactions.



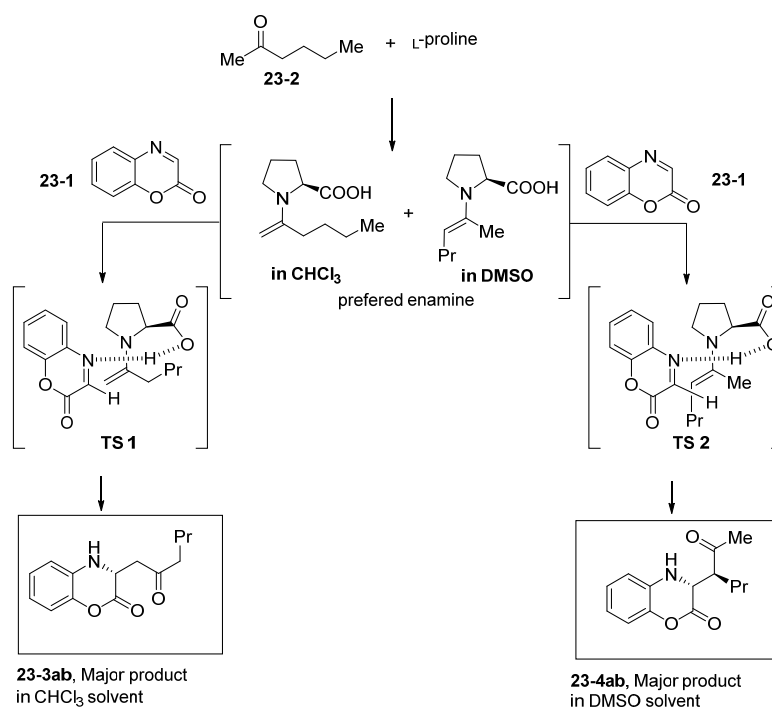
Scheme 44. Possible reaction mechanism for chiral amine-catalyzed asymmetric cycloadditions.

In 2018, we reported an L-proline-catalyzed, solvent-controlled regiodivergent Mannich reaction between cyclic imines and various ketones (Scheme 45) [144]. By utilizing this protocol, a wide range of ketones (**23-2**) and benzoxazinone cyclic imines (**23-1**) effi-

ciently underwent the Mannich reaction in a highly enantio- and diastereoselective manner. Later, a useful α -amino acid derivative was obtained after the removal of the aromatic auxiliary. The use of unsymmetrical ketones as nucleophilic partners, depending on the solvent, enabled different regioselective products to be obtained. Subsequently, highly enantioselective linear isomers were obtained as major products when the reaction was performed in chloroform (**23-3**). This may also proceed via the formation of the a less substituted enamine intermediate (**TS1**). On the other hand, we found that the polar solvent DMSO furnished the branch isomer as the major product, and that this reaction was highly enantio- and diastereoselective (**23-4**). The role of the solvent in the reaction remained unclear. However, other researchers also reportedly observed a similar transition state (**TS2**) when they utilized DMSO as the solvent. The XRD analysis (X-ray diffraction analysis) revealed that the obtained branch isomer was in fact an anti-Mannich adduct, suggesting that the enamine approaches the *Re* face of the benzoxazinone imine (Scheme 46).



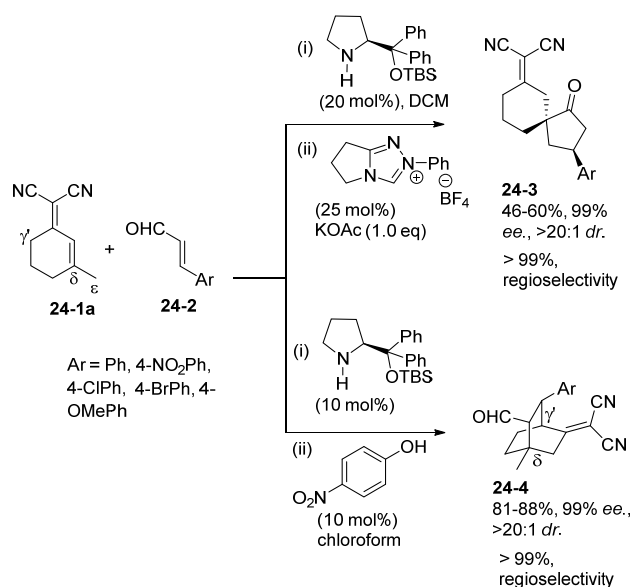
Scheme 45. Solvent-controlled regiodivergent Mannich reaction.



Scheme 46. Plausible reaction mechanism for regiodivergent Mannich reaction.

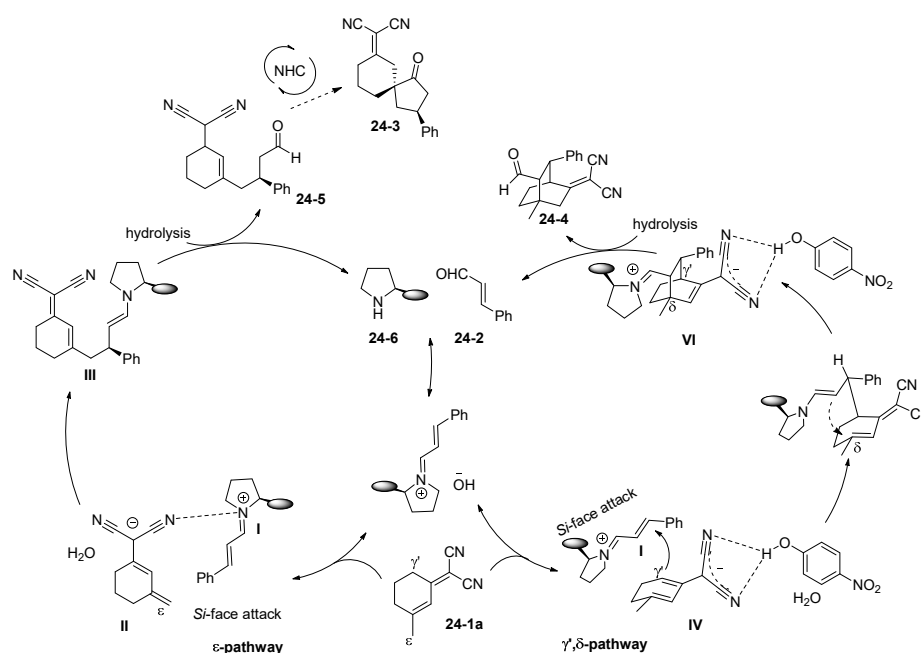
Zanardi *et al.* reported the divergent regio- and stereoselective synthesis of spirodec-anones and bicyclooctane derivatives via [3+2] and [4+2] cycloadditions, respectively (Scheme 47) [145]. The enolizable dicyanodienes (**24-1**) reacted with cinnamaldehyde (**24-**

2) in the presence of an amine/NHC catalyst in a one-pot reaction to afford the spirodec-anone (**24-3**) via a [3+2] cycloaddition reaction. On the other hand, the addition of 4-nitrophenol as a co-catalyst switched the reactivity to produce bicyclooctane carbaldehydes (**24-4**) by a [4+2] cycloaddition. A sequential C- ϵ regioselective bis-vinylogous Michael addition in the presence of a bulky TBS protected the prolinol catalyst, followed by an NHC-catalyzed 1,6-Stetter reaction involving C- δ [3+2] spiroannulation, producing ϵ,δ -bonded spiro[4.5]decanones in the presence of potassium acetate as the base. Substrates of different sizes (including both EWGs and EDGs on the benzene ring) were well tolerated with complete diastereoselectivity (>20:1 *dr*) along with complete regioselectivity and a high enantiomeric excess. A two-step domino reaction sequence was utilized to synthesize bicyclo[2.2.2]octane carbaldehydes via a formal [4+2] cycloaddition reaction. Initially, γ' enolate was formed from the enolizable dicyanodienes and the enal, activated by the prolinol catalyst following which the subsequent intramolecular 1,6-Michael addition at the δ region afforded the expected product. The use of 10 mol% 4-nitrophenol as an additive in chloroform at room temperature afforded the product in good yields with 17:1 site selectivity along with high *ee* (96%) and *dr* (>20:1).



Scheme 47. Regioselective synthesis of enantioenriched carbocyclic compounds.

The reaction mechanism that was proposed (Scheme 48) involves the initial activation of the cinnamaldehyde (**24-2**) by the organocatalyst prolinol silyl ether by lowering the LUMO. Subsequently, the hydroxide ion deprotonates the cyclohexenylidene malononitriles at ϵ,δ' to yield both of the enolates **II** and **IV**, respectively. Coulombic interaction between the enal nitrogen atom and the nitrogen atoms of the cyano group initiates enantioselective attack of the *Si* face of the enal acceptor by the bis-vinylogous enolate **II**. Hydrolysis of enamine intermediate **III** produces **24-5** and, ultimately, the final product **24-3**, and this is accompanied by the regeneration of the organocatalysts. For the [4+2] cycloaddition reaction, the δ' -enolate is not stabilized by the enal nitrogen; instead, it is stabilized by the addition of *p*-nitrophenol, which acts as a hydrogen bond donor. Under these circumstances, the attack of **IV** (from its *Re* face) to the *Si* face of the enal is more favorable, producing bicyclooctane carbaldehydes (**24-4**) upon hydrolysis of intermediate **VI** along with the regeneration of the catalyst.



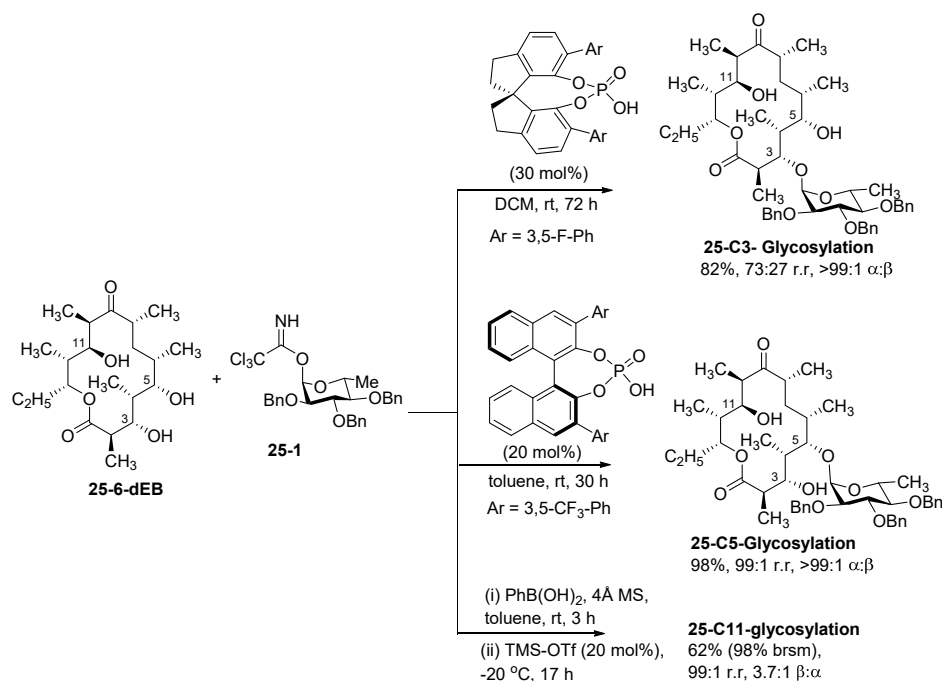
Scheme 48. Proposed reaction mechanism for regiodivergent ϵ - and γ',δ -pathways.

4. Brønsted Acid Catalysts

4.1. Phosphoric Acid Catalysts

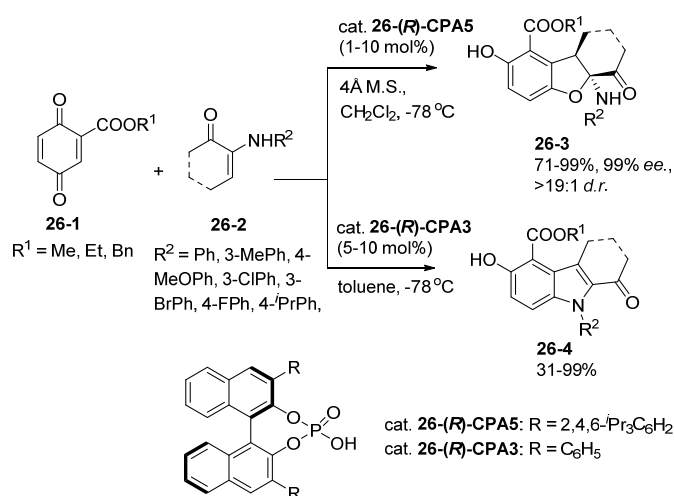
In recent years, the activation of carbonyl compounds by utilizing chiral Brønsted acids has received an enormous amount of attention, i.e., the activation of reactants by way of a hydrogen bonding connection, which is one of the fastest growing research areas. Chiral phosphoric acids have proven to be highly efficient catalysts for a wide range of asymmetric transformations under mild reaction conditions. In general, binaphthyl is used to synthesize chiral phosphoric acid derivatives. These catalysts have been involved in several reactions including the Diels–Alder, Nazarov, Mukaiyama Aldol, Mannich, Henry, Morita–Baylis–Hillman reactions, and 1,3-dipolar cycloadditions [146–154].

Tay and co-workers reported an efficient method for the regioselective synthesis of glycosides in macrolactone (Scheme 49) [155]. Chiral phosphoric acid-catalyzed selective glycosylation of complex phenols was achieved with excellent regiodivergence. Glycosylation of **6-dEB** (**25-6-DEB**) with 6-deoxyglucose (**25-1**) in the presence of BINOL-based chiral phosphoric acids led to glycosylation at the **C5** position of the macrolactone with a high r.r. (regiomeric ratio) (99:01) in toluene. However, the use of SPINOL as a chiral phosphoric acid in DCM resulted in glycosylation at the **C3** alcohol of the macrolactone with a 73:27 r.r. The **C11** hydroxyl was also selectively glycosylated in the presence of phenylboronic acid in toluene as the solvent. The **C3** and **C5** hydroxyls were present in a 1,3-syn relationship, which was masked by the formation of the boronic acid ester to allow formation of the glycoside at the **C11** position. The hydroxyl groups at **C3** and **C5** were regenerated after the boronate was cleaved during the subsequent workup with peroxide.



Scheme 49. Regiodivergent glycosylation of 6-deoxy-erythrionolide B.

In 2020, Wang's group developed aza- and oxo-[3+2] cycloadditions between α -enaminones (**26-2**) and quinones (**26-1**) in the presence of chiral phosphoric acids and 4Å molecular sieves (M.S.), respectively (Scheme 50) [156]. In the presence of the chiral phosphoric acid (**26-(R)-CPA5**), a wide range of *N*-substituted indoles (**26-4**) were obtained as the products of a formal aza-[3+2] cycloaddition. On the other hand, in the presence of bulky chiral phosphoric acid (**26-(R)-CPA3**) and 4Å molecular sieves as an additive, the product 2,3-dihydrobenzofuran (**26-3**) was produced in the highest yields with excellent enantioselectivities via an oxo-[3+2] cycloaddition. Various substituted quinones including different esters (Me, Et, and Bn), and α -enaminones containing an EDG and EWG reacted smoothly to produce the products in good yield with excellent enantioselectivities.



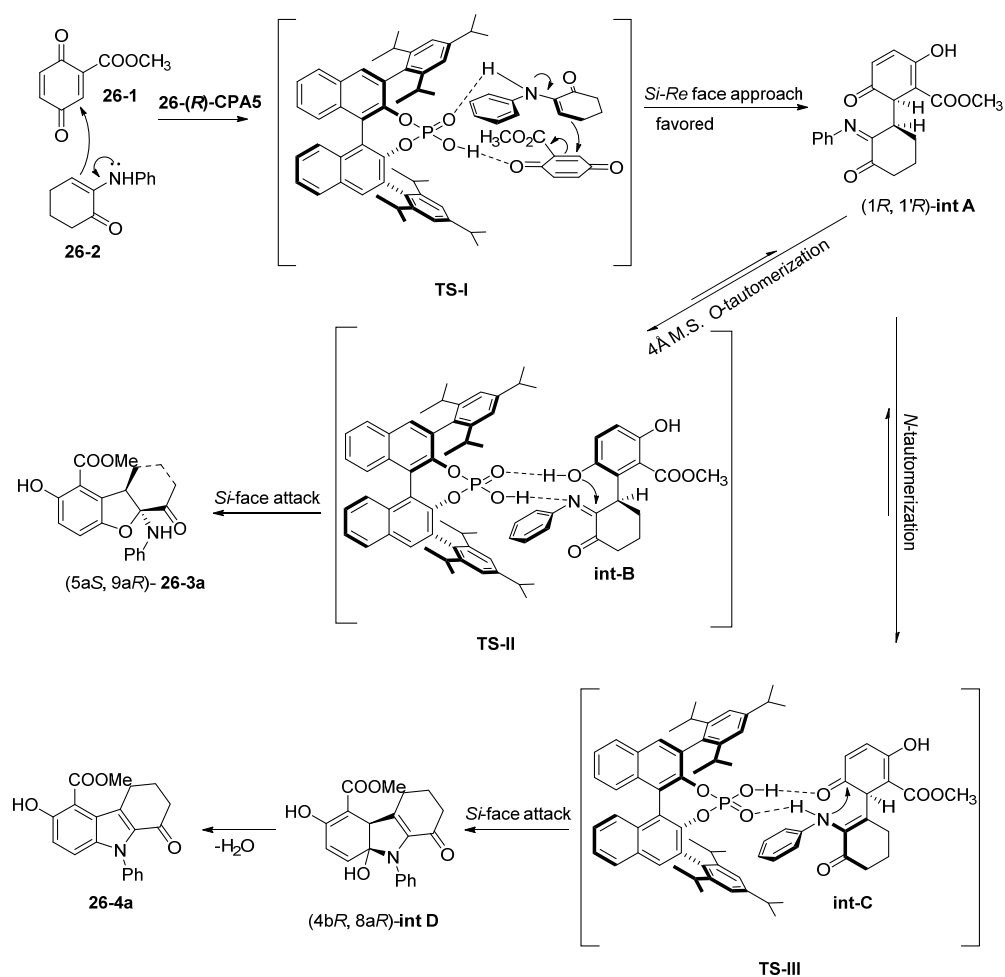
Scheme 50. Formal oxo- and aza-[3+2] reactions of α -enaminones and quinones.

In the absence of molecular sieves, this reaction proceeded to produce *N*-substituted indole derivatives in excellent yield with toluene as the solvent (**26-4**). Quinones containing different ester groups as well as α -enaminones bearing an EDG or EWG at the *para*

position of the aryl ring were compatible under the optimized conditions and delivered the indole derivatives in good yield.

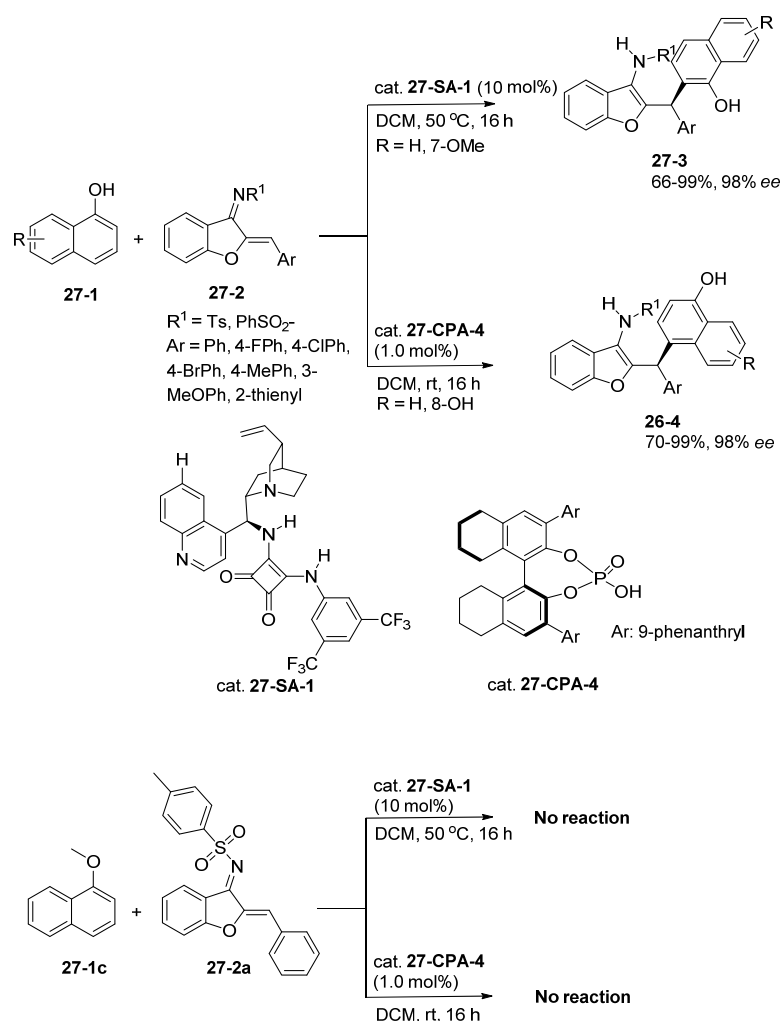
The role of 4Å M.S. was important to obtain benzofuran derivatives. In the absence of molecular sieves, or when they are replaced by dry MgSO_4 or freshly activated 4Å M.S. and H_2O (2μL), this would slow down the formation of benzofuran derivatives (**26-3**) and slightly increase the formation of indole derivatives (**26-4**). These above data reveal that M.S. do not serve as a drying reagent in this reaction, and the addition of water relatively favors the indole formation. Further, the size and format of M.S. also influence the reaction outcome. In detail, for 3Å M.S. and 4Å M.S., their selectivity towards benzofuran and indole is >20:1 (**26-3**:**26-4**), whereas in the case of 5Å M.S., 4Å M.S. (beads), and wet 4Å M.S. (beads), it is about 11:1, 1:1, and 1:5.3, respectively. From ^1H NMR and ^{31}P NMR studies of chiral phosphoric acid with and without M.S., the authors concluded that M.S. could affect the acidity of phosphoric acid and accelerate the interaction between the catalyst and the substrate.

According to the proposed mechanism (Scheme 51), the enamine of the α -enaminones (**26-2**) initially acts as a nucleophile to attack the *Re* face of the quinone (**26-1**) from the *Si* face to afford the intermediate **int-A** via **TS-I**. *O*-tautomerization from the quinone (enol/phenol) and *N*-tautomerization (enamine from the imine) afford **int B** and **int C**, respectively. These intermediates (**int-B**, **int-C**) are attached to the chiral phosphoric acid, as illustrated for **TS-II** and **TS-III**. The hydroxy group of **TS-II** then attacks the *Si* face of the imine to afford 2,3-dihydrobenzofuran (**26-3a**), whereas indole (**26-4a**) is obtained from **TS-III** via **int D**. Initially, the amine group attacks the *Si* face of the carbonyl group to afford **int D**, which then undergoes dehydroxylation to produce the indole derivative. As **TS II** is more polarized in nature than **TS III**, a polar solvent such as DCM stabilizes **TS II**, and the addition of 4Å molecular sieves (4Å M.S.) accelerates the proton transfer in **TS II** via absorbing/releasing a proton. Alternatively, **TS-II** is destabilized in the presence of toluene, a non-polar solvent, in which case the reaction preferentially proceeds via **TS-III**.



Scheme 51. Proposed reaction mechanism for formal oxo- and aza-[3+2] reactions.

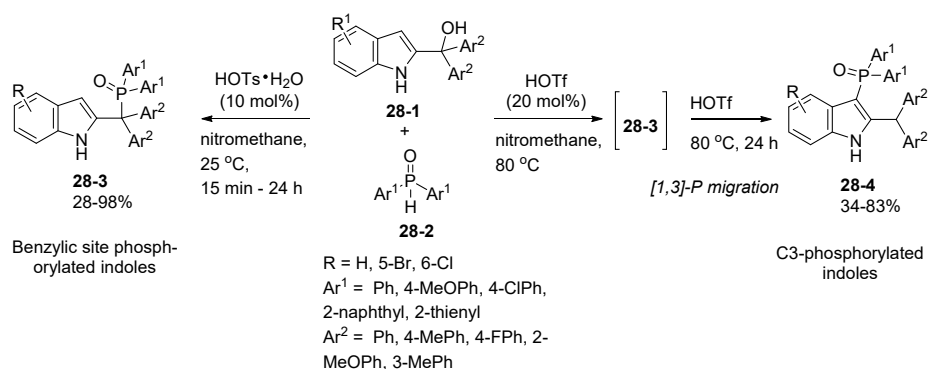
Recently, in 2020, the group of Li and Li reported *ortho*- and *para*-selective regiodivergent C-H functionalization between 1-naphthols (**27-1**) and 1-azadienes (**27-2**) via a Michael addition reaction (Scheme 52) [157]. The chiral squaramide catalyst afforded a product in which an *ortho*-selective C-H bond was constructed, whereas *para*-selective C-H bond formation occurred in the case of chiral phosphoric acid catalysts. Under the optimized reaction conditions, with the chiral squaramide catalyst (**27-SA-1**), 1-naphthol with different substituted 1-azadienes (F, Cl, Br, Me, and OMe) afforded the expected *ortho*-selective Friedel–Crafts alkylation products in good yields with high enantioselectivities (**27-3**). Similar results were obtained with different substituted 1-naphthols (Br, OMe) which delivered the *ortho*-selective products in excellent yields with good *ee*. The use of **27-CPA-4** (1 mol%) as the catalyst resulted in regiodivergent *para*-selective C-H bond functionalization (**27-4**). Within the scope of this substrate, 1-azadienes containing various EWGs (F, Cl, Br) and EDGs (Me, OMe) on the aromatic ring could be well tolerated to offer *para*-selective Friedel–Crafts alkylation products in good yields and with high *ee*. Control experiments showed that the free hydroxy group of 1-naphthol was essential to obtain the product in this Michael addition. Both the catalysts (**27-SA-1**, **27-CPA-4**) failed to produce the product when 1-hydroxynaphthalene was protected with methyl (1-methoxynaphthalene, **27-1c**), which reacts with 1-azadiene (**27-2a**).



Scheme 52. Regiodivergent C-H functionalization of 1-naphthols with 1-azadienes.

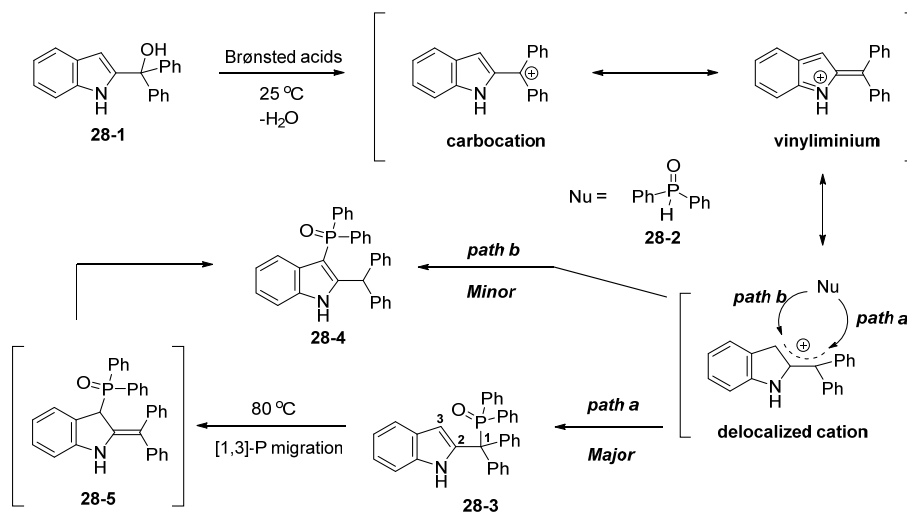
4.2. *p*-Toluenesulfonic Acid Catalyst

Chen and co-workers reported the regiodivergent nucleophilic phosphorylation of indolylmethanols (**28-1**) with diaryl phosphine oxide (**28-2**) in the presence of a Brønsted acid catalyst (Scheme 53) [158]. The benzyl phosphorylated product (**28-3**) was obtained by the utilization of 10 mol% of TsOH.H₂O (*p*-toluenesulfonic acid monohydrate) in nitromethane at 25 °C with moderate to good yield. A variety of 2-indolylmethanols with an EDG produced comparably higher yields than those with an EWG. Similarly, diarylphosphine oxides with an EWG at the *para* position produced higher yields. On the other hand, the C-3 phosphorylation product (**28-4**) was obtained in good yield by using 20 mol% of the TfOH catalyst at 80 °C. Indolylmethanol containing both an EDG and EWG was well tolerated to afford the products in moderate yields.



Scheme 53. Brønsted acid-catalyzed regiodivergent phosphorylation of 2-indolylmethanols.

In the proposed reaction mechanism (Scheme 54), the Brønsted acids generate a partial positive charge at the benzylic position of the nitrogen atom or the C3 position of the 2-indolylmethanols. Then, the diarylphosphine oxides attack the benzylic position to afford the benzylic phosphorylated product **28-3**. In the presence of a strong acid such as TfOH and upon exposure to heat, the benzylic phosphorylated product may undergo a [1,3]-P migration to afford the thermodynamically stable product (**28-4**) via transient intermediate **28-5**. Cross-over experiments concluded that the [1,3]-P migration entailed intramolecular migration. The acidity of the Brønsted acid was a crucial factor because the [1,3]-P migration hardly occurred in the presence of a weak acid.



Scheme 54. Possible reaction pathway for phosphorylation of 2-indolylmethanols.

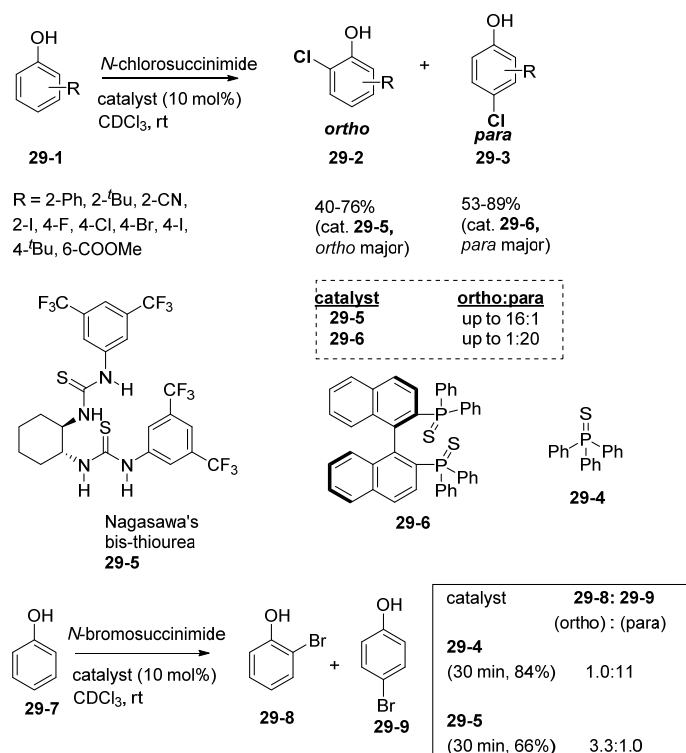
5. Hydrogen Bond-Donating Catalysts

5.1. Thiourea Catalyst

In recent decades, thiourea derivatives have been commonly used as organocatalysts in organic and pharmaceutical chemistry. Moreover, these derivatives are also widely used as bifunctional catalysts in combinations such as amine–thiourea and phosphine–thiourea. Along with their catalytic activity, they are also involved as a component in various reactions including guanylation, thioarylation, and C–S cross-coupling reactions [159–166].

The regiodivergent chlorination of electron-rich phenols (**29-1**) established by Gustafson and co-workers is demonstrated in Scheme 55 [167]. Here, *ortho*-chlorination of the phenol (**29-2**) with *N*-chlorosuccinimide is promoted by 10 mol% of Nagasawa's bis-thiourea catalyst (**29-5**). The *meta*-substituted phenols (F, Cl, Br, I, and *t*-Bu) efficiently afforded good *ortho*-regioselectivity in the presence of Nagasawa's catalyst. The authors also

demonstrated the augmentation of the innate *para*-selectivity of phenols by using BINAP-derived phosphine sulfide as a catalyst (**29-6**). Phenols containing Ph, *t*-Bu, CN, and a halogen substituent afforded a *para*-selective chlorinated product as the major product (**29-3**). The authors also investigated the reaction conditions for regioselective bromination. Catalyst **29-4** afforded mainly the *para*-selective brominated product as the major regioisomer (**29-9**), whereas the presence of Nagasawa's bis-thiourea catalyst overcame the innate *para*-preference of the phenol to afford the *ortho*-brominated products (**29-8**) with good selectivity. The authors concluded that the regioselectivity mainly depends on the structure of the Lewis bases, and reversal of the regioselectivity by Nagasawa's bis-thiourea catalyst could promote chlorination via dual activation. That is, one of the thiourea moieties interacts with the phenol and the other activates NCS via a Lewis base or Brønsted acid manifold.



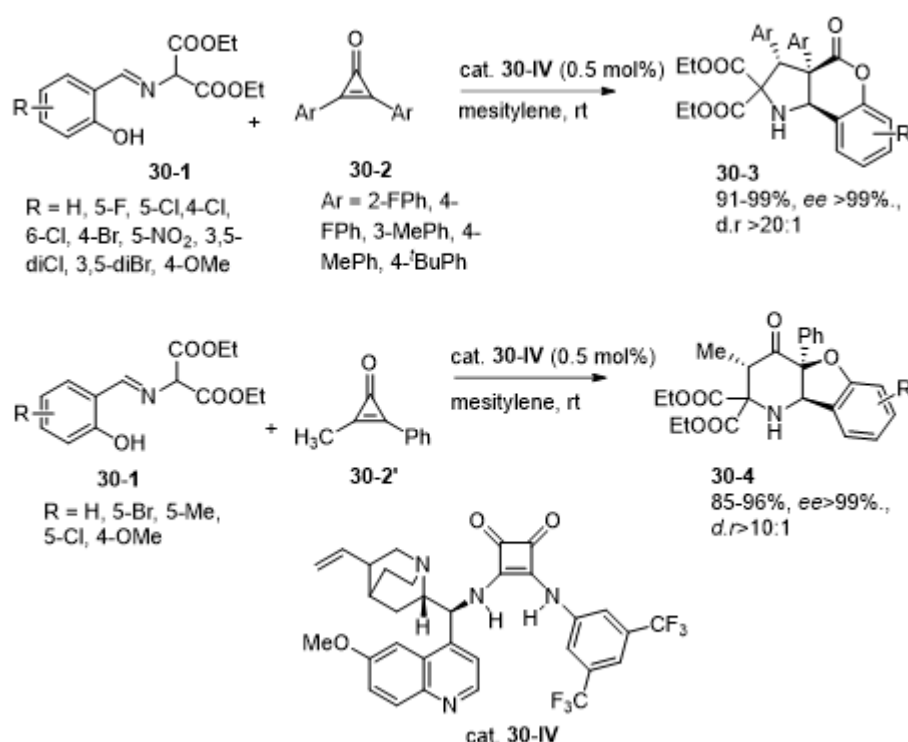
Scheme 55. Catalyst-controlled regiodivergent chlorination of phenols.

5.2. Squaramide Catalyst

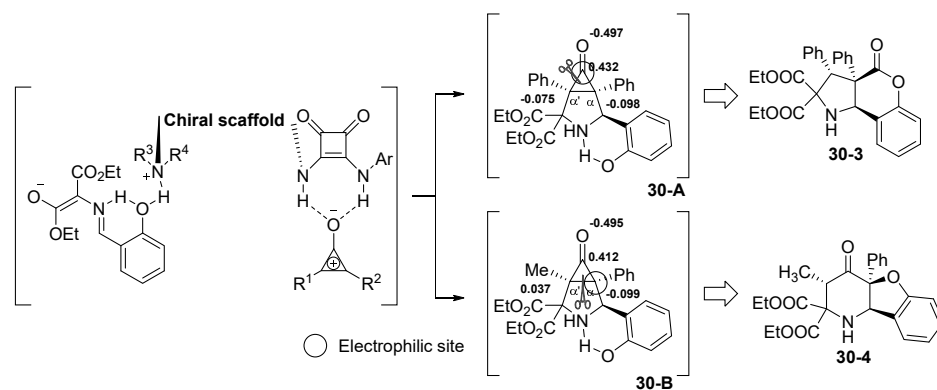
Chiral squaramide, a bifunctional organocatalyst, is an effective alternative for urea/thiourea catalysts. Chiral squaramide has been shown to successfully catalyze several reactions including Michael additions, and the Mannich, aza-Henry, and Strecker reactions. Moreover, these catalysts have successfully produced enantio-enriched products in single and domino/cascade reactions in various asymmetric organic transformations [168–176].

In 2018, Xu and co-workers reported the organocatalytic, regiodivergent C–C bond cleavage of cyclopropenones (Scheme 56) [177]. Their efficient methodology involves a cascade cycloaddition followed by a regioselective cyclopropyl ring strain release process catalyzed by bifunctional squaramide catalysts. Aldimines (**30-1**) reacted with 2,3-diphenylcycloprop-2-enone (**30-2**) with 1 mol% of the catalyst to afford tetrahydrochromeno[4,3-*b*]pyrroles (**30-3**) as products in excellent yields with excellent *ee* and *dr* ratios (20:1). In contrast, completely different cyclized products, tetrahydrobenzofuro[3,2-*b*]pyridines (**30-4**), were obtained when methylphenylcyclopropenone (**30-2'**) was used along with 20 mol% of the catalyst. The products were obtained in excellent yields with

excellent enantioselectivities. The synergistic effect of hydrogen bonding activation and controlled ring strain release played a pivotal role in the generation of the two different ring systems. The “spring-loaded” intermediate with switchable C-C bond cleavages achieved by controllable ring strain release governed the regioselectivity of the reaction (Scheme 57). Nucleophilic addition to the hydroxy group at the carbonyl carbon (**30-A**) produced five-membered products, whereas six-membered cyclic products were obtained when the ring opening occurred at the α -site of the carbonyl carbon (**30-B**). This was substantiated by DFT studies. With this protocol, the authors were able to synthesize diverse heterocyclic frameworks with good enantioselectivity of 99% and an excellent yield (as high as 99%) for both regioisomers.



Scheme 56. Regiodivergent C-C bond cleavage of cyclopropenones.



Scheme 57. Results of the DFT calculation of the Mulliken charge distribution for **30-A** and **30-B**.

6. Conclusions

This review summarized the control of regiodivergent reactions by utilizing various organocatalysts. The use of several organocatalysts such as Lewis bases, amine bases,

Brønsted acids, and hydrogen bond-donating catalysts that were employed to deliver the regiodivergent products was described. The reactivity of various organocatalytic systems, the scope of the substrates, and their mechanistic studies were briefly discussed. The choice of the catalysts, additives, temperature, and solvents was found to play a crucial role in determining the regioselectivity of the reaction.

Although synthetic chemists have devoted lots of efforts to developing organocatalytic regiodivergent methods, in order to cater to the need for diverse molecules to access the chemical space, we need more regiodivergent methods by which we can synthesize a broad range of molecules easily.

Author Contributions: Writing-original draft preparation, review, and editing, M.V. (Mayavan Viji), M.V. (Manjunatha Vishwanath); Writing: S.L.; Chem Draw: J.S., C.J.; Conceptualization and Supervision: H.L.; J.-K.J. All authors have read and agreed to the published version of the manuscript.

Funding: This work was supported by National Research Foundation of Korea grants funded by the Korea government (MSIT) (MRC 2017R1A5A2015541, and 2020R1A2C1007346).

Acknowledgments: The authors thank the valuable help of Hauen Jung, the suggestions and advices with English-writing style

Conflicts of Interest: The authors declare no conflict of interest.

References

1. Xiao, X.; Shao, B.-X.; Lu, Y.-J.; Cao, Q.-Q.; Xia, C.-N.; Chen, F.-E. Recent Advances in Asymmetric Organomulticatalysis. *Adv. Synth. Catal.* **2021**, *363*, 352–387.
2. Milton, J.P.; Fossey, J.S. Azetidines and their applications in asymmetric catalysis. *Tetrahedron* **2021**, *77*, 131767.
3. Das, T.; Mohapatra, S.; Mishra, N.P.; Nayak, S.; Raiguru, B.P. Recent Advances in Organocatalytic Asymmetric Michael Addition Reactions to α , β -Unsaturated Nitroolefins. *ChemistrySelect* **2021**, *6*, 3745–3781.
4. Yin, Y.; Zhao, X.; Qiao, B.; Jiang, Z. Cooperative photoredox and chiral hydrogen-bonding catalysis. *Org. Chem. Front.* **2020**, *7*, 1283–1296.
5. Skrzyńska, A.; Frankowski, S.; Albrecht, Ł. Cyclic 1-Azadienes in the Organocatalytic Inverse-Electron-Demand Aza-Diels-Alder Cycloadditions. *Asian J. Org. Chem.* **2020**, *9*, 1688–1700.
6. Ding, P.-G.; Zhou, F.; Wang, X.; Zhao, Q.-H.; Yu, J.-S.; Zhou, J. H-bond donor-directed switching of diastereoselectivity in the Michael addition of α -azido ketones to nitroolefins. *Chem. Sci.* **2020**, *11*, 3852–3861.
7. He, X.-H.; Ji, Y.-L.; Peng, C.; Han, B. Organocatalytic Asymmetric Synthesis of Cyclic Compounds Bearing a Trifluoromethylated Stereogenic Center: Recent Developments. *Adv. Synth. Catal.* **2019**, *361*, 1923–1957.
8. Liu, Y.; Li, J.; Ye, X.; Zhao, X.; Jiang, Z. Organocatalytic asymmetric formal arylation of benzofuran-2(3H)-ones with cooperative visible light photocatalysis. *Chem. Commun.* **2016**, *52*, 13955–13958.
9. Hernández, J.G.; Juaristi, E. Recent efforts directed to the development of more sustainable asymmetric organocatalysis. *Chem. Commun.* **2012**, *48*, 5396–5409.
10. MacMillan, D.W.C. The advent and development of organocatalysis. *Nature* **2008**, *455*, 304–308.
11. Pellissier, H. Asymmetric organocatalysis. *Tetrahedron* **2007**, *63*, 9267–9331.
12. Mukherjee, S.; Yang, J.W.; Hoffmann, S.; List, B. Asymmetric Enamine Catalysis. *Chem. Rev.* **2007**, *107*, 5471–5569.
13. Erkkilä, A.; Majander, I.; Pihko, P.M. Iminium Catalysis. *Chem. Rev.* **2007**, *107*, 5416–5470.
14. Ahrendt, K.A.; Borths, C.J.; MacMillan, D.W.C. New Strategies for Organic Catalysis: The First Highly Enantioselective Organocatalytic Diels–Alder Reaction. *J. Am. Chem. Soc.* **2000**, *122*, 4243–4244.
15. Tu, M.-S.; Chen, K.-W.; Wu, P.; Zhang, Y.-C.; Liu, X.-Q.; Shi, F. Advances in organocatalytic asymmetric reactions of vinylindoles: Powerful access to enantioenriched indole derivatives. *Org. Chem. Front.* **2021**, *8*, 2643–2672.
16. Laviós, A.; Sanz-Marco, A.; Vila, C.; Blay, G.; Pedro, J.R. Asymmetric Organocatalytic Synthesis of aza-Spirocyclic Compounds from Isothiocyanates and Isocyanides. *Eur. J. Org. Chem.* **2021**, *2021*, 2268–2284.
17. Han, B.; He, X.-H.; Liu, Y.-Q.; He, G.; Peng, C.; Li, J.-L. Asymmetric organocatalysis: An enabling technology for medicinal chemistry. *Chem. Soc. Rev.* **2021**, *50*, 1522–1586.
18. Li, X.; Guo, L.; Peng, C.; Han, B. Organocatalytic Asymmetric Cascade Reactions Based on Gamma-Nitro Carbonyl Compound. *Chem. Rec.* **2019**, *19*, 394–423.
19. Wang, Y.; Cobo, A.A.; Franz, A.K. Recent advances in organocatalytic asymmetric multicomponent cascade reactions for enantioselective synthesis of spirooxindoles. *Org. Chem. Front.* **2021**, *8*, 4315–4348.
20. Wang, L.; Zhu, H.; Peng, T.; Yang, D. Conjugated ynones in catalytic enantioselective reactions. *Org. Biomol. Chem.* **2021**, *19*, 2110–2145.

21. Li, F.; Liang, S.; Luan, Y.; Chen, X.; Zhao, H.; Huang, A.; Li, P.; Li, W. Organocatalytic regio-, diastereo- and enantioselective γ -additions of isoxazol-5(4H)-ones to β,γ -alkynyl- α -imino esters for the synthesis of axially chiral tetrasubstituted α -amino allen-ates. *Org. Chem. Front.* **2021**, *8*, 1243–1248.
22. Guo, X.; Chen, X.; Cheng, Y.; Chang, X.; Li, X.; Li, P. Organocatalytic enantioselective [2 + 4]-annulation of γ -substituted allen-ates with *N*-acyldiazenes for the synthesis of optically active 1,3,4-oxadiazines. *Org. Biomol. Chem.* **2021**, *19*, 1727–1731.
23. Yang, Q.-Q.; Yin, X.; He, X.-L.; Du, W.; Chen, Y.-C. Asymmetric Formal [5 + 3] Cycloadditions with Unmodified Morita–Baylis–Hillman Alcohols via Double Activation Catalysis. *ACS Catal.* **2019**, *9*, 1258–1263.
24. Nanjo, T.; Zhang, X.; Tokuhito, Y.; Takemoto, Y. Divergent and Scalable Synthesis of α -Hydroxy/Keto- β -amino Acid Analogues by the Catalytic Enantioselective Addition of Glyoxylate Cyanohydrin to Imines. *ACS Catal.* **2019**, *9*, 10087–10092.
25. Kostenko, A.A.; Kucherenko, A.S.; Komogortsev, A.N.; Lichitsky, B.V.; Zlotin, S.G. Asymmetric Michael addition between kojic acid derivatives and unsaturated ketoesters promoted by C2-symmetric organocatalysts. *Org. Biomol. Chem.* **2018**, *16*, 9314–9318.
26. He, X.-L.; Zhao, H.-R.; Duan, C.-Q.; Du, W.; Chen, Y.-C. Remote Asymmetric Oxa-Diels–Alder Reaction of 5-Allylic Furfurals via Dearomatizative Tetraenamine Catalysis. *Org. Lett.* **2018**, *20*, 804–807.
27. Bisai, V.; Bisai, A.; Singh, V.K. Enantioselective organocatalytic aldol reaction using small organic molecules. *Tetrahedron* **2012**, *68*, 4541–4580.
28. Terada, M. Chiral Phosphoric Acids as Versatile Catalysts for Enantioselective Transformations. *Synthesis* **2010**, *2010*, 1929–1982.
29. Terada, M. Binaphthol-derived phosphoric acid as a versatile catalyst for enantioselective carbon–carbon bond forming reactions. *Chem. Commun.* **2008**, *35*, 4097–4112.
30. Yang, G.-F.; Li, G.-X.; Huang, J.; Fu, D.-Q.; Nie, X.-K.; Cui, X.; Zhao, J.-Z.; Tang, Z. Regioselective, Diastereoselective, and Enantioselective One-Pot Tandem Reaction Based on an in Situ Formed Reductant: Preparation of 2,3-Disubstituted 1,5-Benzodiazepine. *J. Org. Chem.* **2021**, *86*, 5110–5119.
31. Kutwal, M.S.; Padmaja, V.M.D.; Appayee, C. Regio- and Enantioselective α,γ -Dialkylation of α,β -Unsaturated Aldehydes Through Cascade Organocatalysis. *Eur. J. Org. Chem.* **2020**, *2020*, 2720–2724.
32. Gui, H.-Z.; Meng, Z.; Xiao, Z.-S.; Yang, Z.-R.; Wei, Y.; Shi, M. Stereo- and Regioselective Construction of Spirooxindoles Having Continuous Spiral Rings via Asymmetric [3+2] Cyclization of 3-Isothiocyanato Oxindoles with Thioaurone Derivatives. *Eur. J. Org. Chem.* **2020**, *2020*, 6614–6622.
33. Padmaja, V.M.D.; Jangra, S.; Appayee, C. Highly regioselective α -alkylation of $\alpha,\beta,\gamma,\delta$ -unsaturated aldehydes. *Org. Biomol. Chem.* **2019**, *17*, 1714–1717.
34. Kutwal, M.S.; Dev, S.; Appayee, C. Catalytic Regioselective γ -Methylenation of α,β -Unsaturated Aldehydes Using Formaldehyde via Vinylogous Aldol Condensation. *Org. Lett.* **2019**, *21*, 2509–2513.
35. Xiao, W.; Yang, Q.-Q.; Chen, Z.; Ouyang, Q.; Du, W.; Chen, Y.-C. Regio- and Diastereodivergent [4 + 2] Cycloadditions with Cyclic 2,4-Dienones. *Org. Lett.* **2018**, *20*, 236–239.
36. Kutwal, M.S.; Appayee, C. Highly Regio- and Enantioselective γ -Alkylation of Linear α,β -Unsaturated Aldehydes. *Eur. J. Org. Chem.* **2017**, *2017*, 4230–4234.
37. Hejmanowska, J.; Jasiński, M.; Wojciechowski, J.; Młostoń, G.; Albrecht, L. The first organocatalytic, ortho-regioselective inverse-electron-demand hetero-Diels–Alder reaction. *Chem. Commun.* **2017**, *53*, 11472–11475.
38. Arimitsu, S.; Yonamine, T.; Higashi, M. Cinchona-Based Primary Amine Catalyzed a Proximal Functionalization of Dienamines: Asymmetric α -Fluorination of α -Branched Enals. *ACS Catal.* **2017**, *7*, 4736–4740.
39. Stiller, J.; Marqués-López, E.; Herrera, R.P.; Fröhlich, R.; Strohmman, C.; Christmann, M. Enantioselective α - and γ -Alkylation of α,β -Unsaturated Aldehydes Using Dienamine Activation. *Org. Lett.* **2011**, *13*, 70–73.
40. Guillena, G.; Hita, M.d.C.; Nájera, C. Organocatalyzed direct aldol condensation using L-proline and BINAM-prolinamides: Regio-, diastereo-, and enantioselective controlled synthesis of 1,2-diols. *Tetrahedron Asymmetry* **2006**, *17*, 1027–1031.
41. Kong, X.; Yu, F.; Chen, Z.; Gong, F.; Yang, S.; Liu, J.; Luo, B.; Fang, X. Catalytic chemodivergent annulations between α -diketones and alkynyl α -diketones. *Sci. China Chem.* **2021**, *64*, 991–998.
42. Zhang, J.; Yang, J.-D.; Cheng, J.-P. Diazaphosphinyl radical-catalyzed deoxygenation of α -carboxy ketones: A new protocol for chemo-selective C–O bond scission via mechanism regulation. *Chem. Sci.* **2020**, *11*, 8476–8481.
43. Xiao, Y.; Zhao, J.; Zhao, M.; Chong, R.; Li, X.; Qiao, Y. Mechanism, Chemoselectivity, and Stereoselectivity of NHC-Catalyzed Asymmetric Desymmetrization of Enal-Tethered Cyclohexadienones. *Eur. J. Org. Chem.* **2020**, *2020*, 3726–3733.
44. Boruah, D.J.; Maurya, R.A.; Yuvaraj, P. Chemo-selective Synthesis of [indoline-3,4'-isoxazolo[5,4-b]pyridine Fused spirooxindole Derivatives via Brønsted Acid Catalysed Three-Component Tandem Knoevenagel/Michael Addition Reaction. *Results Chem.* **2020**, *2*, 100064.
45. Beletskaya, I.P.; Nájera, C.; Yus, M. Chemodivergent reactions. *Chem. Soc. Rev.* **2020**, *49*, 7101–7166.
46. Liu, W.; Zou, L.; Fu, B.; Wang, X.; Wang, K.; Sun, Z.; Peng, F.; Wang, W.; Shao, Z. A Multifaceted Directing Group Switching Ynones as Michael Donors in Chemo-, Enantio-, and γ -Selective 1,4-Conjugate Additions with Nitroolefins. *J. Org. Chem.* **2016**, *81*, 8296–8305.
47. Wu, Z.; Wang, X.; Li, F.; Wu, J.; Wang, J. Chemoselective N-Heterocyclic Carbene-Catalyzed Cascade of Enals with Nitroalkenes. *Org. Lett.* **2015**, *17*, 3588–3591.
48. Wang, M.; Rong, Z.-Q.; Zhao, Y. Stereoselective synthesis of ϵ -lactones or spiro-heterocycles through NHC-catalyzed annulation: Divergent reactivity by catalyst control. *Chem. Commun.* **2014**, *50*, 15309–15312.

49. Ping, L.; Chung, D.S.; Bouffard, J.; Lee, S.G. Transition metal-catalyzed site- and regio-divergent C-H bond functionalization. *Chem. Soc. Rev.* **2017**, *46*, 4299–4328.
50. Alam, K.; Hong, S.W.; Oh, K.H.; Park, J.K. Divergent C–H Annulation for Multifused N-Heterocycles: Regio- and Stereospecific Cyclizations of N-Alkynylindoles. *Angew. Chem. Int. Ed.* **2017**, *56*, 13387–13391.
51. Wu, F.-P.; Wu, X.-F. Ligand-Controlled Copper-Catalyzed Regiodivergent Carbonylative Synthesis of α -Amino Ketones and α -Boryl Amides from Imines and Alkyl Iodides. *Angew. Chem. Int. Ed.* **2021**, *60*, 695–700.
52. Jiang, W.-S.; Ji, D.-W.; Zhang, W.-S.; Zhang, G.; Min, X.-T.; Hu, Y.-C.; Jiang, X.-L.; Chen, Q.-A. Orthogonal Regulation of Nucleophilic and Electrophilic Sites in Pd-Catalyzed Regiodivergent Couplings between Indazoles and Isoprene. *Angew. Chem. Int. Ed.* **2021**, *60*, 8321–8328.
53. Li, X.; Liang, G.; Shi, Z.-J. Regio-Divergent C-H Alkynylation with Janus Directing Strategy via Ir(III) Catalysis. *Chin. J. Chem.* **2020**, *38*, 929–934.
54. Kuai, C.-S.; Ji, D.-W.; Zhao, C.-Y.; Liu, H.; Hu, Y.-C.; Chen, Q.-A. Ligand-Regulated Regiodivergent Hydrosilylation of Isoprene under Iron Catalysis. *Angew. Chem. Int. Ed.* **2020**, *59*, 19115–19120.
55. Nájera, C.; Beletskaya, I.P.; Yus, M. Metal-catalyzed regiodivergent organic reactions. *Chem. Soc. Rev.* **2019**, *48*, 4515–4618.
56. Zhan, G.; Du, W.; Chen, Y.-C. Switchable divergent asymmetric synthesis via organocatalysis. *Chem. Soc. Rev.* **2017**, *46*, 1675–1692.
57. Yan, T.; Babu, K.R.; Wu, Y.; Li, Y.; Tang, Y.; Xu, S. Phosphine-Catalyzed Cross-Coupling of Benzyl Halides and Fumarates. *Org. Lett.* **2021**, *23*, 4570–4574.
58. Qi, S.-S.; Yin, H.; Wang, Y.-F.; Wang, C.-J.; Han, H.-T.; Man, T.-T.; Xu, D.-Q. Catalytic Asymmetric Conjugate Addition/Hydroalkoxylation Sequence: Expeditious Access to Enantioenriched Eight-Membered Cyclic Ether Derivatives. *Org. Lett.* **2021**, *23*, 2471–2476.
59. Li, H.; He, Z. Chiral phosphine-catalyzed asymmetric [4 + 1] annulation of polar dienes with allylic derivatives: Enantioselective synthesis of substituted cyclopentenones. *Tetrahedron Lett.* **2021**, *67*, 152863.
60. Chen, G.-S.; Fang, Y.-B.; Ren, Z.; Tian, X.; Liu, Y.-L. Reaction condition-dependent divergent synthesis of spirooxindoles and bisoxindoles. *Org. Chem. Front.* **2021**, *8*, 3820–3828.
61. Zhang, Z.-B.; Yang, Y.; Yu, Z.-X.; Xia, J.-B. Lewis Base-Catalyzed Amino-Acylation of Arylallenes via C–N Bond Cleavage: Reaction Development and Mechanistic Studies. *ACS Catal.* **2020**, *10*, 5419–5429.
62. Deng, Q.; Mu, F.; Qiao, Y.; Wei, D. A theoretical review for novel Lewis base amine/imine-catalyzed reactions. *Org. Biomol. Chem.* **2020**, *18*, 6781–6800.
63. Cheng, C.; Sun, X.; Miao, Z. A PPh₃-catalyzed sequential annulation reaction to construct cyclopentane-fused dihydropyrazolone-pyrrolidinediones. *Org. Biomol. Chem.* **2020**, *18*, 5577–5581.
64. Chen, L.; He, J. DABCO-Catalyzed Michael/Alkylation Cascade Reactions Involving α -Substituted Ammonium Ylides for the Construction of Spirocyclopropyl Oxindoles: Access to the Powerful Chemical Leads against HIV-1. *J. Org. Chem.* **2020**, *85*, 5203–5219.
65. Jin, H.; Dai, C.; Huang, Y. DBU-Catalyzed Desymmetrization of Cyclohexadienones: Access to Vicinal Diamine-Containing Heterocycles. *Org. Lett.* **2018**, *20*, 5006–5009.
66. Guo, H.; Fan, Y.C.; Sun, Z.; Wu, Y.; Kwon, O. Phosphine Organocatalysis. *Chem. Rev.* **2018**, *118*, 10049–10293.
67. Zhang, X.-C.; Cao, S.-H.; Wei, Y.; Shi, M. Phosphine- and Nitrogen-Containing Lewis Base Catalyzed Highly Regioselective and Geometric Selective Cyclization of Isatin Derived Electron-Deficient Alkenes with Ethyl 2,3-Butadienoate. *Org. Lett.* **2011**, *13*, 1142–1145.
68. Lian, Z.; Shi, M. Nitrogen- and Phosphorus-Containing Lewis Base Catalyzed [4+2] and [3+2] Annulation Reactions of Isatins with But-3-yn-2-one. *Eur. J. Org. Chem.* **2012**, *2012*, 581–586.
69. Zhang, Y.; Sun, Y.; Wei, Y.; Shi, M. Phosphine-Catalyzed Intermolecular Annulations of Fluorinated *ortho*-Aminophenones with Alkynones—The Switchable [4+2] or [4+2]/[3+2] Cycloaddition. *Adv. Synth. Catal.* **2019**, *361*, 2129–2135.
70. Gao, X.; Li, Z.; Yang, W.; Liu, Y.; Chen, W.; Zhang, C.; Zheng, L.; Guo, H. Phosphine-catalyzed [3 + 2] and [4 + 2] annulation reactions of ynones with barbiturate-derived alkenes. *Org. Biomol. Chem.* **2017**, *15*, 5298–5307.
71. Cao, Y.-M.; Lentz, D.; Christmann, M. Synthesis of Enantioenriched Bromohydrins via Divergent Reactions of Racemic Intermediates from Anchimeric Oxygen Borrowing. *J. Am. Chem. Soc.* **2018**, *140*, 10677–10681.
72. Wang, T.; Yu, Z.; Hoon, D.L.; Phee, C.Y.; Lan, Y.; Lu, Y. Regiodivergent Enantioselective γ -Additions of Oxazolones to 2,3-Butadienoates Catalyzed by Phosphines: Synthesis of α,α -Disubstituted α -Amino Acids and *N,O*-Acetal Derivatives. *J. Am. Chem. Soc.* **2016**, *138*, 265–271.
73. Wang, M.; Tseng, P.-Y.; Chi, W.-J.; Suresh, S.; Edukondalu, A.; Chen, Y.-R.; Lin, W. Diversity-Oriented Synthesis of Spirocyclohexene Indane-1,3-diones and Coumarin-Fused Cyclopentanes via an Organobase-Controlled Cascade Reaction. *Adv. Synth. Catal.* **2020**, *362*, 3407–3415.
74. Yang, H.-B.; Fan, X.; Wei, Y.; Shi, M. Solvent-controlled nucleophilic trifluoromethylthiolation of Morita–Baylis–Hillman carbonates: Dual roles of DABCO in activating the Zard's trifluoromethylthiolation reagent and the MBH carbonates. *Org. Chem. Front.* **2015**, *2*, 1088–1093.
75. Luo, H.-Y.; Dong, J.-W.; Xie, Y.-Y.; Song, X.-F.; Zhu, D.; Ding, T.; Liu, Y.; Chen, Z.-M. Lewis Base/Brønsted Acid Co-Catalyzed Asymmetric Thiolation of Alkenes with Acid-Controlled Divergent Regioselectivity. *Chem. Eur. J.* **2019**, *25*, 15411–15418.

76. Ni, H.; Yu, Z.; Yao, W.; Lan, Y.; Ullah, N.; Lu, Y. Catalyst-controlled regioselectivity in phosphine catalysis: The synthesis of spirocyclic benzofuranones via regiodivergent [3 + 2] annulations of aurones and an allenolate. *Chem. Sci.* **2017**, *8*, 5699–5704.
77. Dai, X.; Cahard, D. Regio- and Stereocontrolled Nucleophilic Trifluoromethylthiolation of Morita–Baylis–Hillman Carbonates. *Synlett* **2015**, *26*, 40–44.
78. Chen, X.-Y.; Lin, R.-C.; Ye, S. Catalytic [2+2] and [3+2] cycloaddition reactions of allenates with cyclic ketimines. *Chem. Commun.* **2012**, *48*, 1317–1319.
79. Luo, W.; Shao, B.; Li, J.; Song, D.; Yi, X.; Ling, F.; Zhong, W. Divergent synthesis of spirocyclopentene-pyrazolones and pyranol[2,3-*c*]-pyrazoles via Lewis base controlled annulation reactions. *Tetrahedron Lett.* **2019**, *60*, 151206.
80. Sun, F.; Yin, T.; Feng, A.; Hu, Y.; Yu, C.; Li, T.; Yao, C. Base-promoted regiodivergent allylation of *N*-acylhydrazones with Morita–Baylis–Hillman carbonates by tuning the catalyst. *Org. Biomol. Chem.* **2019**, *17*, 5283–5293.
81. Zhang, W.; Wei, S.; Wang, W.; Qu, J.; Wang, B. Catalytic asymmetric construction of C-4 alkenyl substituted pyrazolone derivatives bearing multiple stereoelements. *Chem. Commun.* **2021**, *57*, 6550–6553.
82. Majdecki, M.; Grodek, P.; Jurczak, J. Stereoselective α -Chlorination of β -Keto Esters in the Presence of Hybrid Amide-Based Cinchona Alkaloids as Catalysts. *J. Org. Chem.* **2021**, *86*, 995–1001.
83. Anif Pasha, M.; Peraka, S.; Ramachary, D.B. Catalytic Asymmetric Synthesis of Benzobicyclo[3.2.1]octanes. *Chem. Eur. J.* **2021**, *27*, 10563–10568.
84. Song, X.; Yan, R.-J.; Du, W.; Chen, Y.-C. Asymmetric Dearomative Cascade Multiple Functionalizations of Activated *N*-Alkylpyridinium and *N*-Alkylquinolinium Salts. *Org. Lett.* **2020**, *22*, 7617–7621.
85. Krishna, A.V.; Reddy, G.S.; Gorachand, B.; Ramachary, D.B. Organocatalytic Asymmetric Formal [3+3]-Cycloaddition to Access 2,3-Diazaspiro[4.5]deca-3,6-dien-1-ones. *Eur. J. Org. Chem.* **2020**, *2020*, 6623–6628.
86. Huang, Y.-S.; Song, S.-G.; Ren, L.; Li, Y.-G.; Wu, X. Enantioselective γ -Alkylation of α,β -Unsaturated Aldehydes Using New Cinchona-Based Primary Amine Catalyst. *Eur. J. Org. Chem.* **2019**, *2019*, 6838–6841.
87. Dočekal, V.; Formánek, B.; Císařová, I.; Veselý, J. A formal [4 + 2] cycloaddition of sulfur-containing alkylidene heterocycles with allenic compounds. *Org. Chem. Front.* **2019**, *6*, 3259–3263.
88. Deng, Y.-H.; Chu, W.-D.; Zhang, X.-Z.; Yan, X.; Yu, K.-Y.; Yang, L.-L.; Huang, H.; Fan, C.-A. Cinchona Alkaloid Catalyzed Enantioselective [4 + 2] Annulation of Allenic Esters and *in Situ* Generated *ortho*-Quinone Methides: Asymmetric Synthesis of Functionalized Chromans. *J. Org. Chem.* **2017**, *82*, 5433–5440.
89. Gui, Y.-Y.; Yang, J.; Qi, L.-W.; Wang, X.; Tian, F.; Li, X.-N.; Peng, L.; Wang, L.-X. A cinchona alkaloid catalyzed enantioselective sulfa-Michael/aldol cascade reaction of isoindigos: Construction of chiral bispirooxindole tetrahydrothiophenes with vicinal quaternary spirocenters. *Org. Biomol. Chem.* **2015**, *13*, 6371–6379.
90. Marcelli, T.; Hiemstra, H. Cinchona Alkaloids in Asymmetric Organocatalysis. *Synthesis* **2010**, *2010*, 1229–1279.
91. Cui, X.-Y.; Duan, H.-X.; Zhang, Y.; Wang, Y.-Q. Asymmetric Mannich Reaction of Aryl Methyl Ketones with Cyclic Imines Benzo[e][1,2,3]oxathiazine 2,2-Dioxides Catalyzed by Cinchona Alkaloid-based Primary Amines. *Chem. Asian J.* **2016**, *11*, 3118–3125.
92. Jin, Y.; Chen, D.; Zhang, X.R. Direct Asymmetric anti-Mannich-Type Reactions Catalyzed by Cinchona Alkaloid Derivatives. *Chirality* **2014**, *26*, 801–805.
93. Fan, W.; Kong, S.; Cai, Y.; Wu, G.; Miao, Z. Diastereo- and enantioselective nitro-Mannich reaction of α -substituted nitroacetates to *N*-phosphoryl imines catalyzed by cinchona alkaloid thiourea organocatalysts. *Org. Biomol. Chem.* **2013**, *11*, 3223–3229.
94. Jaiswal, M.K.; Kumar, R.; Singh, S.; Jain, S.; Vanka, K.; Singh, R.P. The Vinylogous Michael Addition of 3-Alkylidene-2-oxindoles to β,γ -Unsaturated α -Keto Esters by Bifunctional Cinchona Alkaloids. *Eur. J. Org. Chem.* **2020**, *2020*, 5690–5694.
95. Yang, M.; Zhang, M.; Wang, Z.; Tang, L.; Chen, W.; Ban, S.; Li, Q. Highly enantioselective Michael addition of pyrazolin-5-ones to nitroolefins catalyzed by cinchona alkaloid derived 4-methylbenzoylthioureas. *Chirality* **2018**, *30*, 1096–1104.
96. Cabanillas, A.; Davies, C.D.; Male, L.; Simpkins, N.S. Highly enantioselective access to diketopiperazines via cinchona alkaloid catalyzed Michael additions. *Chem. Sci.* **2015**, *6*, 1350–1354.
97. Shao, Y.D.; He, X.Y.; Han, D.D.; Yang, X.R.; Yao, H.B.; Cheng, D.J. Asymmetric Aza-Henry Reaction of Indolenines Mediated by a Cinchona-Alkaloid-Thiourea Organocatalyst. *Asian J. Org. Chem.* **2019**, *8*, 2023–2026.
98. Lu, N.; Fang, Y.; Gao, Y.; Wei, Z.; Cao, J.; Liang, D.; Lin, Y.; Duan, H. Bifunctional Thiourea-Ammonium Salt Catalysts Derived from Cinchona Alkaloids: Cooperative Phase-Transfer Catalysts in the Enantioselective Aza-Henry Reaction with Ketimines. *J. Org. Chem.* **2018**, *83*, 1486–1492.
99. Majdecki, M.; Tyszka-Gumkowska, A.; Jurczak, J. Highly Enantioselective Epoxidation of α,β -Unsaturated Ketones Using Amide-Based Cinchona Alkaloids as Hybrid Phase-Transfer Catalysts. *Org. Lett.* **2020**, *22*, 8687–8691.
100. Berkessel, A.; Guixà, M.; Schmidt, F.; Neudörfl, J.M.; Lex, J. Highly enantioselective epoxidation of 2-methylnaphthoquinone (vitamin K3) mediated by new cinchona alkaloid phase-transfer catalysts. *Chem. Eur. J.* **2007**, *13*, 4483–4498.
101. Cheng, C.; Sun, X.; Wu, Z.; Liu, Q.; Xiong, L.; Miao, Z. Lewis base catalyzed regioselective cyclization of allene ketones or α -methyl allene ketones with unsaturated pyrazolones. *Org. Biomol. Chem.* **2019**, *17*, 3232–3238.
102. Yu, J.-K.; Chien, H.-W.; Lin, Y.-J.; Karanam, P.; Chen, Y.-H.; Lin, W. Diversity-oriented synthesis of chromenopyrrolidines from azomethine ylides and 2-hydroxybenzylidene indandiones *via* base-controlled regiodivergent (3+2) cycloaddition. *Chem. Commun.* **2018**, *54*, 9921–9924.
103. Yang, H.-B.; Wan, D.-H. C–C Bond Acylation of Oxime Ethers via NHC Catalysis. *Org. Lett.* **2021**, *23*, 1049–1053.

104. Yadav, S.; Suresh, S. N-Heterocyclic Carbene (NHC)-Catalyzed Intramolecular Stetter Reaction to Access Dibenzo-fused Seven-membered Heterocycles. *Asian J. Org. Chem.* **2021**, *10*, 1406–1409.
105. Wang, C.; Liu, L. NHC-catalyzed oxindole synthesis via single electron transfer. *Org. Chem. Front.* **2021**, *8*, 1454–1460.
106. Suresh, P.; Thamotharan, S.; Selva Ganesan, S. NHC Organocatalysis in D₂O for the Highly Diastereoselective Synthesis of Deuterated Spiropyran Analogues. *ChemistrySelect* **2021**, *6*, 2036–2040.
107. Song, R.; Jin, Z.; Chi, Y.R. NHC-catalyzed covalent activation of heteroatoms for enantioselective reactions. *Chem. Sci.* **2021**, *12*, 5037–5043.
108. Singh, A.; Narula, A.K. N-Heterocyclic carbene (NHC) catalyzed amidation of aldehydes with amines *via* the tandem N-hydroxysuccinimide ester formation. *New J. Chem.* **2021**, *45*, 7486–7490.
109. Satyam, K.; Ramarao, J.; Suresh, S. N-Heterocyclic carbene (NHC)-catalyzed intramolecular benzoin condensation–oxidation. *Org. Biomol. Chem.* **2021**, *19*, 1488–1492.
110. Leng, H.; Zhao, Q.; Mao, Q.; Liu, S.; Luo, M.; Qin, R.; Huang, W.; Zhan, G. NHC-catalysed retro-aldol/aldol cascade reaction enabling solvent-controlled stereodivergent synthesis of spirooxindoles. *Chin. Chem. Lett.* **2021**, in press, doi:10.1016/j.ccl.2021.03.009.
111. Barman, D.; Ghosh, T.; Show, K.; Debnath, S.; Ghosh, T.; Maiti, D.K. NHC-Mediated Stetter-Aldol and Imino-Stetter-Aldol Domino Cyclization to Naphthalen-1(2H)-ones and Isoquinolines. *Org. Lett.* **2021**, *23*, 2178–2182.
112. Barik, S.; Biju, A.T. N-Heterocyclic carbene (NHC) organocatalysis using aliphatic aldehydes. *Chem. Commun.* **2020**, *56*, 15484–15495.
113. Wu, Q.; Li, C.; Wang, W.; Wang, H.; Pan, D.; Zheng, P. NHC-catalyzed enantioselective synthesis of dihydropyran-4-carbonitriles bearing all-carbon quaternary centers. *Org. Chem. Front.* **2017**, *4*, 2323–2326.
114. Gould, E.; Walden, D.M.; Kasten, K.; Johnston, R.C.; Wu, J.; Slawin, A.M.Z.; Mustard, T.J.L.; Johnston, B.; Davies, T.; Ha-Yeon Cheong, P.; et al. Catalyst selective and regiodivergent O- to C- or N-carboxyl transfer of pyrazolyl carbonates: Synthetic and computational studies. *Chem. Sci.* **2014**, *5*, 3651–3658.
115. Campbell, C.D.; Joannesse, C.; Morrill, L.C.; Philp, D.; Smith, A.D. Regiodivergent Lewis base-promoted O- to C-carboxyl transfer of furanyl carbonates. *Org. Biomol. Chem.* **2015**, *13*, 2895–2900.
116. Yu, C.; Shen, S.; Jiang, L.; Li, J.; Lu, Y.; Li, T.; Yao, C. NHC-catalyzed regiodivergent syntheses of difunctionalized 3-pyrazolidinones from α -bromoaldehyde and monosubstituted hydrazine. *Org. Biomol. Chem.* **2017**, *15*, 9149–9155.
117. Guo, C.; Sahoo, B.; Daniliuc, C.G.; Glorius, F. N-Heterocyclic Carbene Catalyzed Switchable Reactions of Enals with Azoalkenes: Formal [4 + 3] and [4 + 1] Annulations for the Synthesis of 1,2-Diazepines and Pyrazoles. *J. Am. Chem. Soc.* **2014**, *136*, 17402–17405.
118. Guo, C.; Fleige, M.; Janssen-Müller, D.; Daniliuc, C.G.; Glorius, F. Switchable selectivity in an NHC-catalysed dearomatizing annulation reaction. *Nat. Chem.* **2015**, *7*, 842–847.
119. Sun, Z.; Zha, T.; Shao, Z. Enantiodivergent synthesis of tricyclic chromans: Remote nucleophilic groups switch selectivity in catalytic asymmetric cascade reactions of trifunctional substrates. *Green Synth. Catal.* **2021**, *2*, 241–245.
120. Chen, Z.-C.; Du, W.; Chen, Y.-C. New Amines and Activation Modes in Asymmetric Aminocatalysis. *Chin. J. Chem.* **2021**, *39*, 1775–1786.
121. da Silva, A.F.; Leonarczyk, I.A.; Ferreira, M.A.B.; Jurberg, I.D. Diastereodivergent aminocatalyzed spirocyclization strategies using 4-alkylideneisoxazol-5-ones and methyl vinyl ketones. *Org. Chem. Front.* **2020**, *7*, 3599–3607.
122. Arimitsu, S.; Gima, E. Improvement of primary-amine-catalyzed asymmetric α -benzyloxylation of α -branched enals by a synergistic effect of water and sulfonic acids. *Tetrahedron Lett.* **2020**, *61*, 152032.
123. Przydacz, A.; Skrzyńska, A.; Albrecht, Ł. Breaking Aromaticity with Aminocatalysis: A Convenient Strategy for Asymmetric Synthesis. *Angew. Chem. Int. Ed.* **2019**, *58*, 63–73.
124. Maity, S.; Sar, S.; Ghorai, P. Primary Aminothiourethane-Catalyzed Enantioselective Synthesis of Rauhut–Currier Adducts of 3-Arylcyclohexenone with a Tethered Enone on the Aryl Moiety at the Ortho-Position. *Org. Lett.* **2018**, *20*, 1707–1711.
125. Cui, L.; You, Y.E.; Mi, X.; Luo, S. Asymmetric Fluorination of α -Branched Aldehydes by Chiral Primary Amine Catalysis: Reagent-Controlled Enantioselectivity Switch. *J. Org. Chem.* **2018**, *83*, 4250–4256.
126. Vicario, J.L. Aminocatalytic Enantioselective Cycloadditions. *Synlett* **2016**, *27*, 1006–1021.
127. List, B. Proline-catalyzed asymmetric reactions. *Tetrahedron* **2002**, *58*, 5573–5590.
128. List, B.; Lerner, R.A.; Barbas, C.F. Proline-catalyzed direct asymmetric aldol reactions. *J. Am. Chem. Soc.* **2000**, *122*, 2395–2396.
129. Vesely, J.; Rios, R.; Córdova, A. Proline and Lewis base co-catalyzed addition of α,β -unsaturated aldehydes to nitrostyrenes. *Tetrahedron Lett.* **2008**, *49*, 1137–1140.
130. Córdova, A.; Notz, W.; Barbas, C.F. Proline-Catalyzed One-Step Asymmetric Synthesis of 5-Hydroxy-(2E)-hexenal from Acetaldehyde. *J. Org. Chem.* **2002**, *67*, 301–303.
131. Ramachary, D.B.; Barbas, C.F. Direct Amino Acid-Catalyzed Asymmetric Desymmetrization of meso-Compounds: Tandem Aminooxylation/O–N Bond Heterolysis Reactions. *Org. Lett.* **2005**, *7*, 1577–1580.
132. Watanabe, S.-I.; Córdova, A.; Tanaka, F.; Barbas, C.F. One-Pot Asymmetric Synthesis of β -Cyanohydroxymethyl α -Amino Acid Derivatives: Formation of Three Contiguous Stereogenic Centers. *Org. Lett.* **2002**, *4*, 4519–4522.
133. Juaristi, E. Recent developments in next generation (S)-proline-derived chiral organocatalysts. *Tetrahedron* **2021**, *88*, 132143.
134. Jessen, N.I.; Bertuzzi, G.; Bura, M.; Skipper, M.L.; Jørgensen, K.A. Enantioselective Construction of the Cycl[3.2.2]azine Core via Organocatalytic [12 + 2] Cycloadditions. *J. Am. Chem. Soc.* **2021**, *143*, 6140–6151.

135. Hutchinson, G.; Alamillo-Ferrer, C.; Burés, J. Mechanistically Guided Design of an Efficient and Enantioselective Aminocatalytic α -Chlorination of Aldehydes. *J. Am. Chem. Soc.* **2021**, *143*, 6805–6809.
136. Vachan, B.S.; Karuppasamy, M.; Vinoth, P.; Vivek Kumar, S.; Perumal, S.; Sridharan, V.; Menéndez, J.C. Proline and its Derivatives as Organocatalysts for Multi-Component Reactions in Aqueous Media: Synergic Pathways to the Green Synthesis of Heterocycles. *Adv. Synth. Catal.* **2020**, *362*, 87–110.
137. Vega-Peñaloza, A.; Paria, S.; Bonchio, M.; Dell'Amico, L.; Companyó, X. Profiling the Privileges of Pyrrolidine-Based Catalysts in Asymmetric Synthesis: From Polar to Light-Driven Radical Chemistry. *ACS Catal.* **2019**, *9*, 6058–6072.
138. Gao, X.-Y.; Yan, R.-J.; Xiao, B.-X.; Du, W.; Albrecht, L.; Chen, Y.-C. Asymmetric Formal Vinylogous Iminium Ion Activation for Vinyl-Substituted Heteroaryl and Aryl Aldehydes. *Org. Lett.* **2019**, *21*, 9628–9632.
139. Kumar, P.; Sharma, B.M. Proline-Catalyzed Asymmetric α -Amination in the Synthesis of Bioactive Molecules. *Synlett* **2018**, *29*, 1944–1956.
140. Klier, L.; Tur, F.; Poulsen, P.H.; Jørgensen, K.A. Asymmetric cycloaddition reactions catalysed by diarylprolinol silyl ethers. *Chem. Soc. Rev.* **2017**, *46*, 1080–1102.
141. Donslund, B.S.; Johansen, T.K.; Poulsen, P.H.; Halskov, K.S.; Jørgensen, K.A. The Diarylprolinol Silyl Ethers: Ten Years After. *Angew. Chem. Int. Ed.* **2015**, *54*, 13860–13874.
142. Yang, J.W.; Chandler, C.; Stadler, M.; Kampen, D.; List, B. Proline-catalysed Mannich reactions of acetaldehyde. *Nature* **2008**, *452*, 453–455.
143. Zhou, Z.; Wang, Z.-X.; Zhou, Y.-C.; Xiao, W.; Ouyang, Q.; Du, W.; Chen, Y.-C. Switchable regioselectivity in amine-catalysed asymmetric cycloadditions. *Nat. Chem.* **2017**, *9*, 590–594.
144. Viji, M.; Sim, J.; Li, S.; Lee, H.; Oh, K.; Jung, J.-K. Organocatalytic and Regiodivergent Mannich Reaction of Ketones with Benzoxazinones. *Adv. Synth. Catal.* **2018**, *360*, 4464–4469.
145. Dell'Amico, L.; Rassu, G.; Zambrano, V.; Sartori, A.; Curti, C.; Battistini, L.; Pelosi, G.; Casiraghi, G.; Zanardi, F. Exploring the Vinylogous Reactivity of Cyclohexenylidene Malononitriles: Switchable Regioselectivity in the Organocatalytic Asymmetric Addition to Enals Giving Highly Enantioenriched Carbabicyclic Structures. *J. Am. Chem. Soc.* **2014**, *136*, 11107–11114.
146. Zhang, J.; Liu, M.; Huang, M.; Liu, H.; Yan, Y.; Zhang, X. Enantioselective [3 + 2] annulation of 3-hydroxymaleimides with quinone monoimines. *Org. Chem. Front.* **2021**, *8*, 2268–2273.
147. Varlet, T.; Masson, G. Enamides and dienamides in phosphoric acid-catalysed enantioselective cycloadditions for the synthesis of chiral amines. *Chem. Commun.* **2021**, *57*, 4089–4105.
148. Liu, H.; Yan, Y.; Li, M.; Zhang, X. An enantioselective aza-Friedel–Crafts reaction of 5-aminoisoxazoles with isatin-derived *N*-Boc ketimines. *Org. Biomol. Chem.* **2021**, *19*, 3820–3824.
149. Koay, W.L.; Mei, G.-J.; Lu, Y. Facile access to benzofuran-fused tetrahydropyridines via catalytic asymmetric [4 + 2] cycloaddition of aurone-derived 1-azadienes with 3-vinylindoles. *Org. Chem. Front.* **2021**, *8*, 968–974.
150. Gao, Y.-Q.; Hou, Y.; Chen, J.; Zhen, Y.; Xu, D.; Zhang, H.; Wei, H.; Xie, W. Asymmetric synthesis of 9-alkyl tetrahydroxanthrones via tandem asymmetric Michael/cyclization promoted by chiral phosphoric acid. *Org. Biomol. Chem.* **2021**, *19*, 348–354.
151. Wu, S.-F.; Tu, M.-S.; Hang, Q.-Q.; Zhang, S.; Ding, H.; Zhang, Y.-C.; Shi, F. Construction of chiral chroman scaffolds via catalytic asymmetric (4 + 2) cyclizations of para-quinone methide derivatives with 3-vinylindoles. *Org. Biomol. Chem.* **2020**, *18*, 5388–5399.
152. Varlet, T.; Gelis, C.; Retailleau, P.; Bernadat, G.; Neuville, L.; Masson, G. Enantioselective Redox-Divergent Chiral Phosphoric Acid Catalyzed Quinone Diels–Alder Reactions. *Angew. Chem. Int. Ed.* **2020**, *59*, 8491–8496.
153. Liu, H.; Yan, Y.; Zhang, J.; Liu, M.; Cheng, S.; Wang, Z.; Zhang, X. Enantioselective dearomative [3+2] annulation of 5-aminoisoxazoles with quinone monoimines. *Chem. Commun.* **2020**, *56*, 13591–13594.
154. Li, F.; Zhang, C.; Cheng, Y.; Jia, Q.; Li, W.; Liu, K.; Li, P. Enantioselective Construction of Vicinal Sulfur-functionalized Quaternary and Tertiary Stereocenters via Organocatalytic Michael Addition of 5*H*-Thiazol-4-ones to 1-Azadienes. *Asian J. Org. Chem.* **2020**, *9*, 1183–1186.
155. Tay, J.-H.; Argüelles, A.J.; DeMars, M.D.; Zimmerman, P.M.; Sherman, D.H.; Nagorny, P. Regiodivergent Glycosylations of 6-Deoxy-erythronolide B and Oleandomycin-Derived Macrolactones Enabled by Chiral Acid Catalysis. *J. Am. Chem. Soc.* **2017**, *139*, 8570–8578.
156. Luo, W.; Sun, Z.; Fernando, E.H.N.; Nesterov, V.N.; Cundari, T.R.; Wang, H. Formal oxo- and aza-[3 + 2] reactions of α -enaminones and quinones: A double divergent process and the roles of chiral phosphoric acid and molecular sieves. *Chem. Sci.* **2020**, *11*, 9386–9394.
157. Zhang, C.; Cheng, Y.; Li, F.; Luan, Y.; Li, P.; Li, W. Organocatalytic Enantioselective Regiodivergent C–H Bond Functionalization of 1-Naphthols with 1-Azadienes. *Adv. Synth. Catal.* **2020**, *362*, 1286–1291.
158. Chen, L.; Zou, Y.-X.; Fang, X.-Y.; Wu, J.; Sun, X.-H. Brønsted acid-catalysed regiodivergent phosphorylation of 2-indolylmethanols to synthesize benzylic site or C3-phosphorylated indole derivatives. *Org. Biomol. Chem.* **2018**, *16*, 7417–7424.
159. Marcantonio, E.; Curti, C.; Battistini, L.; Sartori, A.; Cardinale, L.; Pelosi, G.; Zanardi, F. Direct, Asymmetric Synthesis of Carbocycle-Fused Uracils via [4+2] Cycloadditions: A Noncovalent Organocatalysis Approach. *Adv. Synth. Catal.* **2021**, *363*, 2625–2633.
160. Chen, Z.; Zhang, T.; Sun, Y.; Wang, L.; Jin, Y. Organocatalytic enantioselective aza-Friedel–Crafts alkylation of β -naphthols and isatin-derived ketimines via a Takemoto-type catalyst. *New J. Chem.* **2021**, *45*, 10481–10487.
161. Sun, B.-B.; Chen, J.-B.; Zhang, J.-Q.; Yang, X.-P.; Lv, H.-P.; Wang, Z.; Wang, X.-W. Organo-catalyzed asymmetric cascade annulation reaction for the construction of bi-spirocyclic pyrazolone and oxindole derivatives. *Org. Chem. Front.* **2020**, *7*, 796–809.

162. Rodríguez-Rodríguez, M.; Maestro, A.; Andrés, J.M.; Pedrosa, R. Supported Bifunctional Chiral Thioureas as Catalysts in the Synthesis of 3-Amino-2-Oxindoles through Enantioselective aza-Friedel-Crafts Reaction: Application in Continuous Flow Processes. *Adv. Synth. Catal.* **2020**, *362*, 2744–2754.
163. da Silva, T.L.; Rambo, R.S.; Jacoby, C.G.; Schneider, P.H. Asymmetric Michael reaction promoted by chiral thiazolidine-thiourea catalyst. *Tetrahedron* **2020**, *76*, 130874.
164. Yang, X.; Zhou, Y.-H.; Yang, H.; Wang, S.-S.; Ouyang, Q.; Luo, Q.-L.; Guo, Q.-X. Asymmetric Diels–Alder Reaction of 3-Vinylindoles and Nitroolefins Promoted by Multiple Hydrogen Bonds. *Org. Lett.* **2019**, *21*, 1161–1164.
165. Rodríguez-Ferrer, P.; Sanz-Novio, M.; Maestro, A.; Andrés, J.M.; Pedrosa, R. Synthesis of Enantioenriched 3-Amino-3-Substituted Oxindoles by Stereoselective Mannich Reaction Catalyzed by Supported Bifunctional Thioureas. *Adv. Synth. Catal.* **2019**, *361*, 3645–3655.
166. Andrés, J.M.; Maestro, A.; Valle, M.; Pedrosa, R. Chiral Bifunctional Thioureas and Squaramides and Their Copolymers as Recoverable Organocatalysts. Stereoselective Synthesis of 2-Substituted 4-Amino-3-nitrobenzopyrans and 3-Functionalized 3,4-Diamino-4H-Chromenes. *J. Org. Chem.* **2018**, *83*, 5546–5557.
167. Maddox, S.M.; Dinh, A.N.; Armenta, F.; Um, J.; Gustafson, J.L. The Catalyst-Controlled Regiodivergent Chlorination of Phenols. *Org. Lett.* **2016**, *18*, 5476–5479.
168. Yuan, W.-C.; Lei, C.-W.; Zhao, J.-Q.; Wang, Z.-H.; You, Y. Organocatalytic Asymmetric Cyclopropanation of 3-Acylcoumarins with 3-Halooxindoles: Access to Spirooxindole-cyclopropa[c]coumarin Compounds. *J. Org. Chem.* **2021**, *86*, 2534–2544.
169. Liu, Y.; Zhang, Y.; Huang, Q.-W.; Gou, C.; Li, Q.-Z.; Dai, Q.-S.; Leng, H.-J.; Li, J.-L. Organocatalytic Enantioselective Synthesis of Tetrahydro-Furanyl Spirooxindoles via [3+2] Annulations of 3-Hydroxyoxindoles and Cyclic Ketolactams. *Adv. Synth. Catal.* **2021**, *363*, 2177–2182.
170. Biswas, A.; Ghosh, A.; Shankhdhar, R.; Chatterjee, I. Squaramide Catalyzed Asymmetric Synthesis of Five- and Six-Membered Rings. *Asian J. Org. Chem.* **2021**, *10*, 1345–1376.
171. Xu, K.; Chen, W.; Chen, X.; Wang, B.; Huang, J.; Tian, X. Organocatalytic asymmetric Friedel–Crafts alkylation/hemiketalization/lactonization cascade reactions: Highly enantioselective synthesis of furo[2,3-*b*]benzofuranones. *Org. Chem. Front.* **2020**, *7*, 1679–1684.
172. Wen, J.-B.; Du, D.-M. Squaramide-catalysed asymmetric cascade reactions of 2,3-dioxopyrrolidines with 3-chlorooxindoles. *Org. Biomol. Chem.* **2020**, *18*, 1647–1656.
173. Wang, Y.; Du, D.-M. Highly Diastereo- and Enantioselective Synthesis of Isoxazolone-Spirooxindoles via Squaramide-Catalyzed Cascade Michael/Michael Addition Reactions. *J. Org. Chem.* **2020**, *85*, 15325–15336.
174. Hou, X.-Q.; Du, D.-M. Recent Advances in Squaramide-Catalyzed Asymmetric Mannich Reactions. *Adv. Synth. Catal.* **2020**, *362*, 4487–4512.
175. Zhao, X.; Xiong, J.; An, J.; Yu, J.; Zhu, L.; Feng, X.; Jiang, X. Diastereodivergent construction of bispiro[oxindole-bi-pyrrolidine]s with four consecutive stereocenters via asymmetric [3 + 2] cycloaddition of 2,3-dioxopyrrolidines using identical catalysts. *Org. Chem. Front.* **2019**, *6*, 1989–1995.
176. Zhao, B.-L.; Li, J.-H.; Du, D.-M. Squaramide-Catalyzed Asymmetric Reactions. *Chem. Rec.* **2017**, *17*, 994–1018.
177. Cao, J.; Fang, R.; Liu, J.-Y.; Lu, H.; Luo, Y.-C.; Xu, P.-F. Organocatalytic Regiodivergent C–C Bond Cleavage of Cyclopropanones: A Highly Efficient Cascade Approach to Enantiopure Heterocyclic Frameworks. *Chem. Eur. J.* **2018**, *24*, 18863–18867.